12-1-2018

Investigation of ERG1A Potassium Channel Modulation of Calpain Activity in C2C12 Myotubes

Clayton Alan Whitmore
Southern Illinois University Carbondale, claytonw726@gmail.com

INVESTIGATION OF ERG1A POTASSIUM CHANNEL MODULATION OF CALPAIN ACTIVITY IN C2C12 MYOTUBES

by
Clayton Whitmore

A.S., Lincoln Land Community College, 2013
B.S., Illinois State University, 2015

A Thesis
Submitted in Partial Fulfillment of the Requirements for the
Master of Science Degree

Department of Molecular Biology, Microbiology, and Biochemistry
in the Graduate School
Southern Illinois University Carbondale
December 2018

THESIS APPROVAL

INVESTIGATION OF ERG1A POTASSIUM CHANNEL MODULATION OF CALPAIN ACTIVITY IN C2C12 MYOTUBES

By

Clayton Whitmore

A Thesis Submitted in Partial

Fulfillment of the Requirements

for the Degree of

Master of Science

in the field of Molecular Biology, Microbiology, and Biochemistry

Approved by:

Dr. Amber L. Pond, Co-Chair

Dr. Judith K. Davie, Co-Chair

Dr. Rod Weilbaecher

Graduate School
Southern Illinois University Carbondale
October 25, 2018

AN ABSTRACT OF THE THESIS OF

Clayton Whitmore, for the Master of Science degree in Molecular Biology, Microbiology, Biochemistry, presented on October 25, 2018, at Southern Illinois University Carbondale.

TITLE: INVESTIGATION OF ERG1A POTASSIUM CHANNEL MODULATION OF CALPAIN ACTIVITY IN C2C12 MYOTUBES

MAJOR PROFESSORS: Drs. Amber Pond and Judy Davie

Skeletal muscle atrophy is a result of an imbalance in protein synthesis and protein degradation. It is a part of the normal aging process, but also may occur in response to several stimuli including disease, injury, and disuse. Currently there is no truly effective pharmacological treatment for atrophy. The best treatment is a healthy diet and exercise, however, sick and aging individuals are not always capable of participating in the appropriate activity. Therefore, exploration of the mechanisms contributing to atrophy is essential because this may lead to discovery of an effective therapeutic target. The ether-a-go-go related gene (*Erg1a*) K^+ channel has been shown to contribute to atrophy by up-regulating ubiquitin proteasome proteolysis in mice. Recent studies have shown that it also increases the intracellular calcium concentration in skeletal muscle. The aim of this work is to investigate the modulation of the increased intracellular [Ca^{2+}] and its potential downstream effects on calpain activity. To do this, we overexpressed human *ERG1A* (*HERG1A*) in a mouse myoblast cell line (C2C12 cells). Looking for the source of increased calcium levels we investigated the skeletal muscle specific, voltage gated calcium channel (*CAV1.1*). We were able to discover that

there is a significant 2.3 fold increase in Cav1.1 gene expression. Conversely, upon immunoblotting the protein abundance of Cav1.1 had no detectable change. Calpains, which are calcium activated cysteine proteases take part in the degradation of myofilaments when they are activated via calcium. The activity of these calpains were shown to have a 25.7% higher level of activity in response to *HERG* expression. The change in calpain activity may be attributable to increased calpain transcription, translation or changes in their inhibitor, calpastatin. When gene expression was analyzed for calpains and calpastatin, no significant change was observed. However, after analysis of protein abundance a decrease was found in calpains 2 and 3, along with calpastatin, suggesting that HERG1A may indeed be effecting calpain abundance. With our data we were able to conclude that the increase in intracellular [Ca^{2+}] due to the presence of HERG1A is not due to Cav1.1. We were able to report that an increase in calpain activity occurred in response to HERG1A within C2C12 cells, however this was not due to changes in gene expression, but their protein abundance appears to decrease in response to HERG1A.

ACKNOWLEDGMENTS

First, I would like to thank my advisor Dr. Amber Pond for her guidance and motivation. I am grateful for her time in teaching and mentoring me not only in research practices, but also life lessons.

I also thank my committee members co-chair Dr. Judy Davie and Dr. Rod Weilbaecher for their advice and the knowledge they have shared with me. My lab mate, Luke Anderson, thank you for all the hard work you put into research assisting Dr. Pond and I, and keeping the lab running effectively and efficiently on a daily basis. A thank you also to Dr. Gregory Hockerman of Purdue University and his lab, Evan Pratt, Emily Rantz, and Amy Salyer for their assistance. I would like to show my appreciation to all of my friends I have met and worked alongside for your help, kindness, and friendship, I will never forget the memories we have all shared together.

Most of all, I would like to thank my family: my mother, father, stepfather, brothers, sister, cousins, aunts and uncles. You all have been with me through the highs and lows, and I would never be where I am today without your love and support; all that I have accomplished I owe to you.

TABLE OF CONTENTS

LIST OF TABLES

LIST OF FIGURES

FIGURE PAGE

CHAPTER 1

INTRODUCTION

Skeletal muscle comprises approximately 40% of the total human body weight and contains 50-75% of all bodily proteins. It has multiple functions within the human body. It converts chemical energy into mechanical energy that can then be used to support body posture and generate force and movement for everyday activities [1]. It contributes to basal energy metabolism and maintains the core body temperature while consuming the majority of oxygen and fuel used in the body. It also functions to store substrates for both energy production and cell growth (e.g., carbohydrates and amino acids) [1] . Thus, an adequate amount of skeletal muscle tissue is necessary for good health and a reduction in skeletal muscle tissue will compromise health, potentially inhibiting the body's ability to respond to illness and stress [1] . Growth of skeletal muscle occurs by the process of myogenesis, in which myoblasts fuse together to form multinucleated myofibers. This growth process is maintained by a continuous, fluctuating balance between protein degradation and protein synthesis; however, when the rate of degradation increases or the rate of protein synthesis decreases muscle mass can be lost in a process known as atrophy. Skeletal muscle atrophy is defined as a decrease (equal to or greater than 5%) in muscle mass as a result of cellular shrinkage [2]. Indeed, certain external stimuli can interfere with the correct balance between protein synthesis and degradation and cause fully formed muscle cells to degrade at an accelerated rate. Muscle disuse, denervation, starvation, disease (e.g., diabetes and cancer), loss of neural input, along with the normal aging process are a

few of the events that can induce muscle atrophy [3]. Treatments for skeletal muscle atrophy currently under study include administration of pharmaceuticals such as growth factors [4], beta-agonists [5], inhibitors of proteolysis [6, 7], stimulators of protein synthesis [8] and myostatin inhibitors [9-11]; however, these are not adequately effective. Thus, further investigation into the mechanisms resulting in atrophy is needed to reveal new and improved targets for therapy.

The contractile subunit of skeletal muscle is called the sarcomere (Figure 1). The sarcomere is primarily composed of myofilaments, namely actin and myosin (thin and thick filaments, respectively), which function to produce muscle contraction. Other proteins often referred to as “anchoring” proteins assist in stabilizing the sarcomere, these include titin, nebulin, α- actinin, and desmin [1]. Titin is an elastic protein that attaches to the Z disc and helps align and stabilize myosin. Nebulin is often referred to as actin’s “ruler” because it stabilizes actin, being approximately the same length as this filament. The α-actinin protein is found on the Z disc and serves as an anchoring point for actin to this structure. Lastly, desmin is a protein that lies along the Z disc and connects this structure with the sarcolemma and extracellular matrix (Figure 1) [1]. Contraction occurs when the myosin head “pulls” itself along the actin filament causing interdigitation of the actin and myosin filaments (Figure 1); proteins found along the actin filament known as troponin and tropomyosin produce this activity. Tropomyosin lies on the actin protein and blocks the binding sites on actin for the myosin heavy chain head. Troponin lies on top of the tropomyosin. Once Ca^{2+} is released from the sarcoplasmic reticulum in response to an action potential, troponin binds calcium and this binding changes the conformation of tropomyosin to expose the myosin head

binding sites on the actin (Figure 2) [1]. Myosin may then bind actin repeatedly like a ratchet, causing the interdigitating of the filaments and thus contraction. The degradation of these thin and thick contractile filaments is the primary cause of skeletal muscle atrophy; thus, reduction of actin and myosin proteins will lead to reduced muscle mass and strength.

There are three primary proteolytic systems that can contribute to atrophy when active: the ubiquitin proteasome pathway (UPP), cathepsins, and calpains. The UPP has been reported to be the primary pathway that is responsible for the protein degradation that produces skeletal muscle atrophy. It consists of a series of enzymes which activate ubiquitin and attach it to target proteins, and a proteasome unit which degrades the ubiquitinated proteins [3]. Cathepsins, which are a type of cysteine protease, are secreted into the cytosol from the lysosome and initiate the lysosomal pathway to assist in the degradation of proteins [12]. Lastly, calpains, which are the focus of our study, are calcium activated cysteine proteases that are active during atrophic conditions. Specifically, we have focused on the conventional calpains, 1 and 2, along with the skeletal muscle specific, calpain 3. Finally, we have also focused on calpastatin, which is a native protein inhibitor of the conventional calpains [13].

Calpains are detected throughout the body and participate in various processes, including embryonic development and cell function, intracellular signaling, regulation of gene expression, modulation of the cell cycle, and even apoptosis [14]. Increases in calcium increase calpain activity. In skeletal muscle, calpains have been shown to act upon anchoring proteins (e.g., titin, nebulin, and desmin), which attach the sarcomere's myofilaments to the Z-disc [15]. The cleavage of these proteins subsequently releases

α-actinin and thus results in the release of the actin thin filament from the myofibril. Thus, the activation of calpains assists in the degradation of myofibers and the release of their constituent myofilaments (actin and myosin), allowing these proteins to be ubiquinated and consequently degraded by the proteasome [15, 16]. Calpains are additionally known to aid in modulation of signaling pathways. For example, the Akt pathway is known to modulate the balance of protein synthesis and degradation and studies have shown that increased calpain activity will decrease the activity of Akt. The decrease in Akt allows for a decrease in mTOR kinase activity, which contributes to up-regulated protein synthesis. Decreased Akt activity also leads to an increase in the abundances of proteins FoxO1, 3 and GSK-3ß which, when present, lead to protein degradation. Thus, increased calpain activity results in a decrease in protein synthesis and an increase in protein degradation (Figure 3) [16]. The role of calpains does not end there. They have also been shown to degrade tropomyosin and troponin proteins, however, at a much slower rate than anchoring proteins [15]. Combined with the cleavage of titin, this degradation allows the removal of the thick filament from the myofibril. It is important to note that calpains do not cleave proteins into amino acids; rather they cleave specific proteins into large fragments [7]. Thus, calpain activity allows for the disassembly of the sarcomere, allowing actin and myosin to become accessible for ubiquitination and subsequent degradation by the proteasome [15-17].

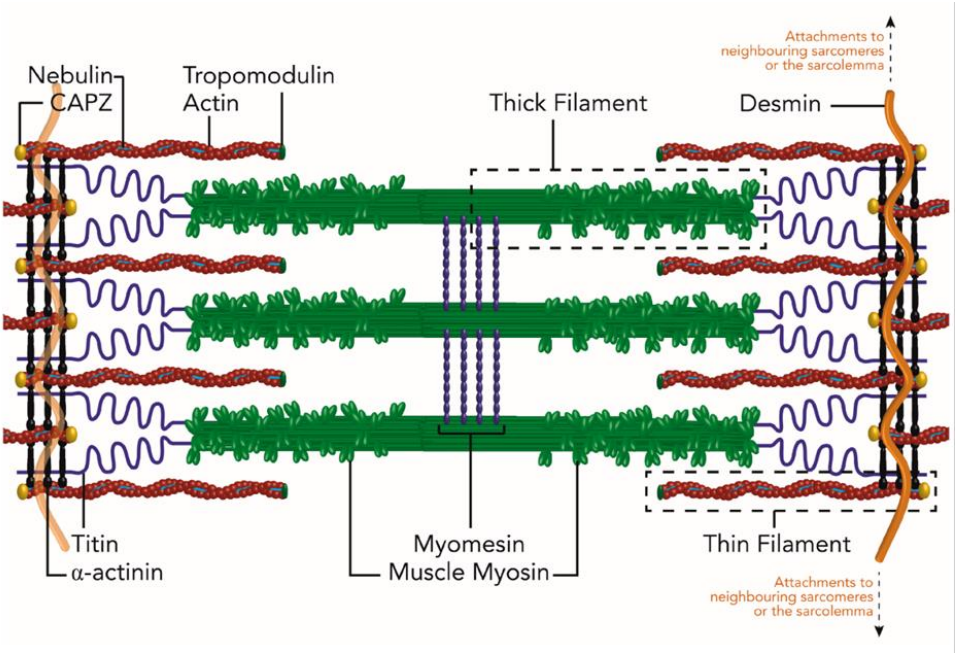

Figure 1. Organization of proteins within a sarcomere [18].

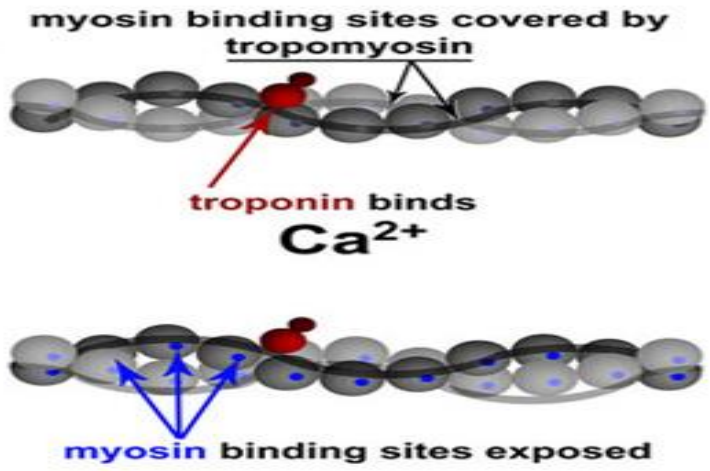

Figure 2. When bound with calcium troponin changes conformation and shifts the tropomyosin protein to expose myosin binding sites on actin, allowing the myosin head to pull itself along the actin filament [19].

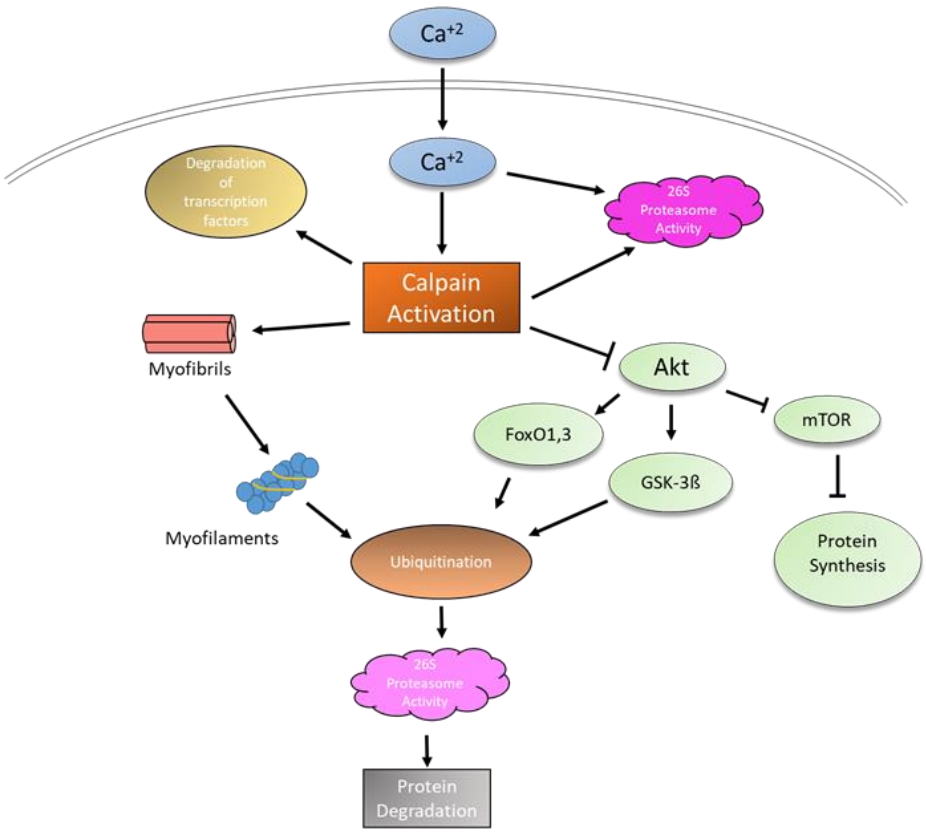

Figure 3. Some consequences of calpain activation.

The ERG1 voltage-gated potassium channel alpha subunit is a product of the ERG1 (*ether-a-go-go related gene*) gene, which is located on chromosome 7 in humans and spans approximately 33 kb. The gene encodes 15 exons and has three alternative transcription start sites along with two alternative termination sites, which allows for five unique transcripts (Figure 4) [20]. The ERG1a protein has six membrane-spanning domains, a conserved pore domain, and an N-terminus with numerous potential signaling domains such as a cyclic nucleotide-binding domain and a Per-Arnt-Sim (PAS) domain (Figure 5A) [20, 21]. The alternative splice variant ERG1b subunit is essentially identical to the 1a variant except that is has a truncated N-terminus. The 1b is considered to be a cardiac specific isoform [20, 21], although there are reports of its

detection in brain and cancer cells [22, 23]. The main difference between the 1b variant and others is that the ERG1b lacks the first 373 amino acids found in 1a, and rather contains its own unique 36 amino acid sequence at the NH_2 terminus [20, 21]. The ERG1 channel is a heteromultimer composed of four alpha subunits. Interestingly, it has been shown that the cardiac ERG1 channel is composed of two ERG1a proteins and two ERG1b proteins [21] while the skeletal muscle channel is solely composed of the ERG1a variant which will be the focus of this study [24].

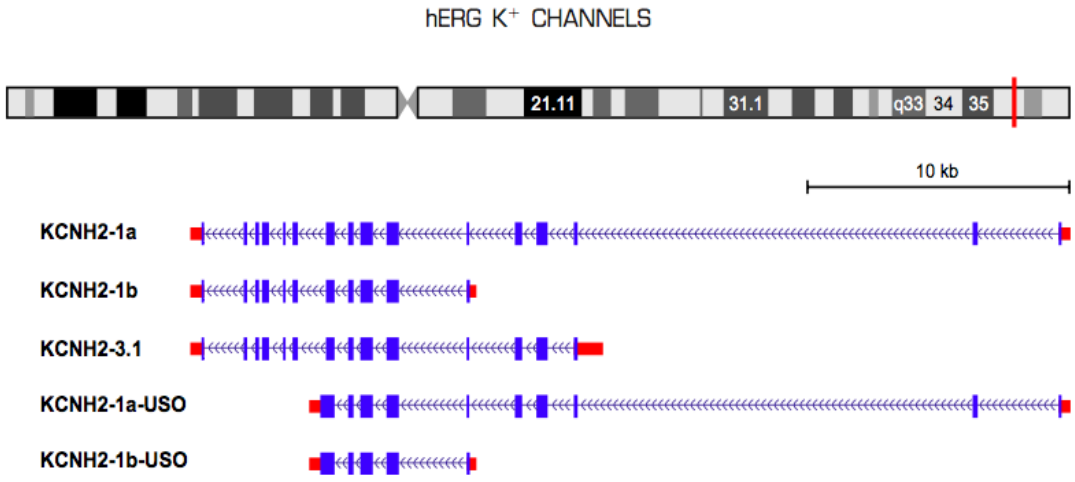

Figure 4. Genomic structure of chromosome 7 including the location of the *ERG* gene (top, red line). The 5 transcript variants of *ERG* result from alternative transcription start and termination sites (bottom). Blue boxes indicate exon-coding regions, red areas signify 5' and 3' UTRs, and blue arrows represent introns [20].

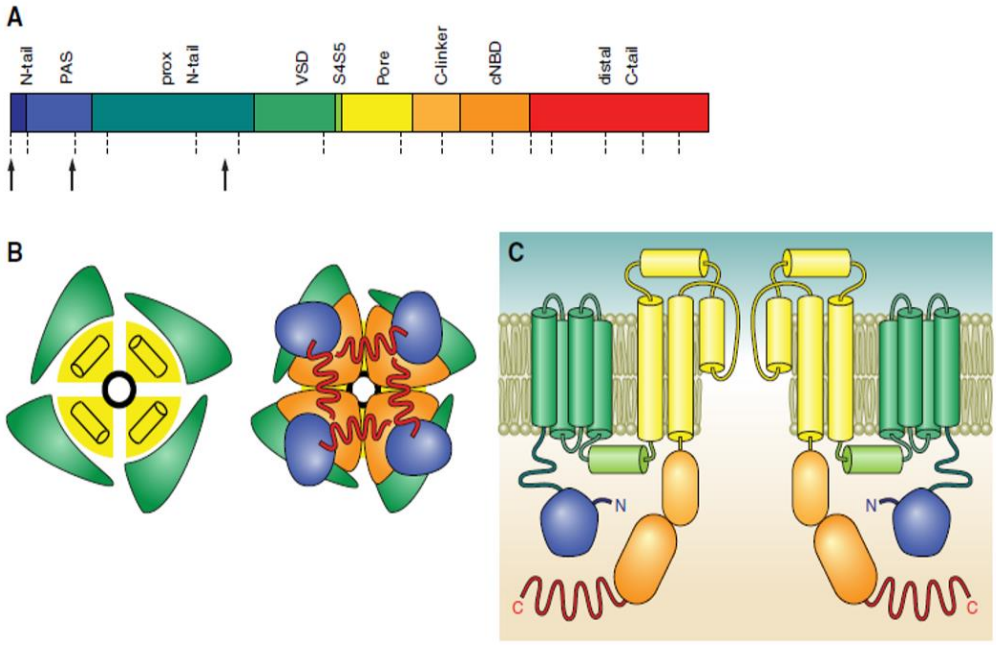

Figure 5. (A) Linear sequence of the HERG1A channel with domains color-coded. Dotted lines represent exon-exon junctions while arrows represent transcription start sites. **(B)** Extracellular view of the HERG1A channel (left) and intracellular view (right) color-coded to match the linear sequence in A. **(C)** Topology of two HERG1A subunits once again color-coded to match panels A and B [20].

ERG1 is well conserved across many mammalian tissues including brain and heart, but had not been reported in skeletal muscle until the report from the Pond and Hannon labs [24]. Within heart tissue the ERG1 potassium channel has been shown to conduct the I_{Kr} current and be partially responsible for the repolarization of the cardiac action potential [20, 21, 25]. Indeed, mutations found in human *ERG1* (HERG1) can produce a form of long QT syndrome, (LQT2) an arrhythmia brought about by prolonged repolarization of the cardiac action potential that can lead to sudden cardiac death.

In 2006, the Pond and Hannon labs demonstrated that ERG1a expression and protein abundance increases in the skeletal muscle of mice in response to hind limb suspension and with tumor expression. Indeed, when ectopically expressed in the skeletal muscle of weight bearing mice, mouse ERG1a (MERG1A) was shown to induce atrophy. Further, when ERG1a was either pharmacologically or genetically blocked, the skeletal muscle atrophy normally caused by hind limb suspension was inhibited [24]. Specifically, they reported that the MERG1A protein increased in *Gastrocnemius* muscles after 4 days of hind limb suspension (i.e., unweighting), prior to the onset of significant atrophy, and was still up-regulated after 7 days of hind limb suspension when significant atrophy was noted. They also reported that the MERG1A channel was up-regulated in the skeletal muscle of cachectic mice. They further demonstrated that genetic and pharmacologic attenuation of MERG1A channel activity prevented atrophy in suspended mice and that expression of *Merg1a* was found to induce a decrease in cross sectional area of muscle fibers in weight bearing mice. Most importantly their findings concluded that the MERG1A channel participates in the initiation of atrophy by signaling for an increase in UPP activity [24].

More than half of the skeletal muscle wasting that occurs in response to immobilization has been shown to be caused by the UPP pathway (Figure 6). Specifically, this pathway is composed of three main enzymes (E1, E2, and E3) and a proteolytic unit called the proteasome. E1 is an ubiquitin-activating enzyme which allows ubiquitin to be attached to ATP and then passed along to E2, which is known as the ubiquitin-conjugating enzyme. E3 ligases are the final enzymes and these transfer ubiquitin to the targeted protein substrate by ligation. Polyubiquitination of a substrate

makes it a target for degradation by the proteasome [2, 15, 26]. MURF1 and *Mafbx*/ATROGIN1 are two muscle specific E3 ligases and are known to be up regulated in atrophic muscle [3]. ERG1a has since been shown to modulate the expression of the E3 ligase MURF1, however, it does not modulate expression of the E3 ligase *Mafbx*/ATROGIN1. This suggests that ERG1a participates in the process of skeletal muscle atrophy at least partially through modulation of the ubiquitin proteasome pathway [25].

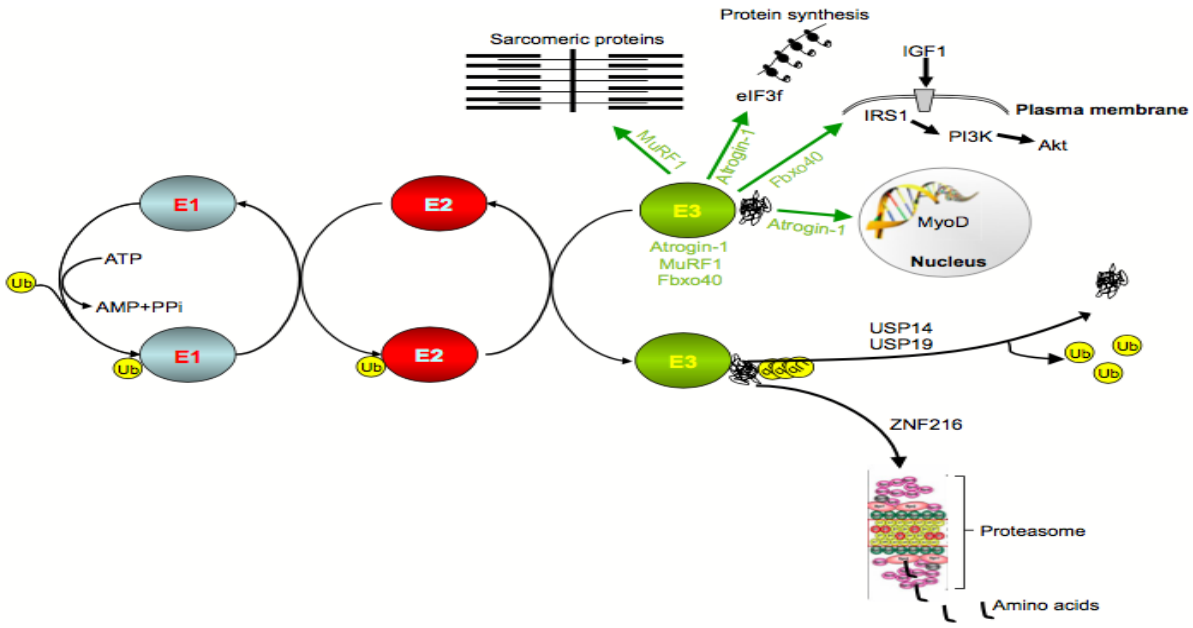

Figure 6. The ubiquitin proteasome pathway [2].

Calcium has multiple roles in skeletal muscle. One of the primary roles is initiation of excitation-contraction coupling (ECC) which requires μM concentrations of calcium ions; however, at nM concentrations calcium also acts as a second messenger in cell signaling systems, modulating the expression of genes needed for growth and differentiation [27-30]. Two different types of calcium transients have been identified in

skeletal muscle, a fast and a slow component. The initial fast calcium release is linked to contraction while the second slow calcium release shows a response to depolarization that is unrelated to ECC. This slow release of calcium in response to depolarization results from an increase in inositol 1,4,5-triphosphate (IP_3) [27]. IP_3 binds to its receptor (IP_3R) and leads to calcium release into the cytosol from the sarcoplasmic reticulum (SR). This calcium is then taken back into the SR via SERCA. The activation of the IP_3R consequently leads to the slow calcium component [27, 31]. The slow calcium transient brought on by depolarization and the consequent increase in IP_3 have been linked to activation of early genes in skeletal muscle, specifically *c-fos, c-jun, egr-1* along with P-ERK (MAPK/ERK pathway) and the cAMP response element-binding protein (P-CREB) [29].

Human ERG1A (HERG1A) has been shown to increase the basal intracellular calcium concentration ($[Ca^{2+}]i$) of SKBr3 breast cancer cells [32]. Indeed the Pond and Hockerman labs have also shown that HERG1A expression will increase the basal $[Ca^{2+}]i$ of C2C12 myotubes as well as produce a transient increase in the $[Ca^{2+}]i$ of myotubes in response to depolarization (Figure 7, unpublished data, Pratt, Hockerman, Pond). However, the mechanism by which the HERG1A channel has this effect is not known. Indeed, we hypothesized that HERG1A expression would increase calpain activity in C2C12 myotubes as a result of the increased calcium concentration. Here, we perform studies designed to explore this hypothesis and the possible consequences of increased calcium activity in the C2C12 myotubes.

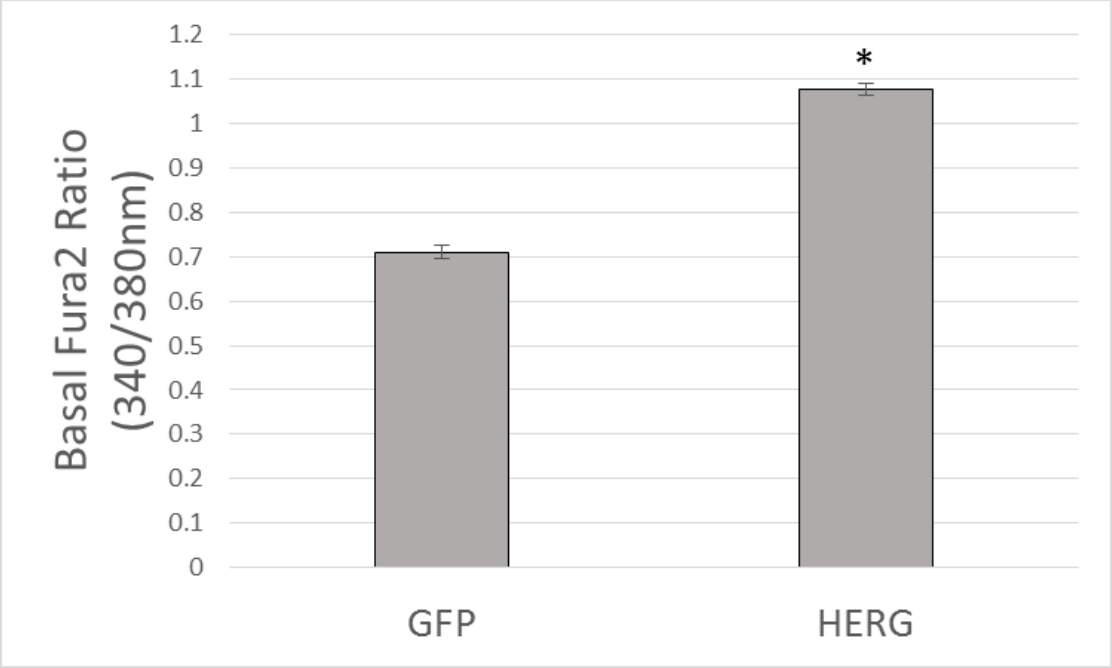

Figure 7. Fura2 dye experiments (340/380nm ratio) reveals a 34% increase in basal intracellular calcium levels ($[Ca^{2+}]i$) in HERG1A transduced cells as opposed to GFP transduced control cells. ($p<0.0001$; n=90 control, n=87 HERG1A). Bars represent the mean while error bars represent the standard error from mean (mean ± SEM) (unpublished data, Pratt, Hockerman, and Pond).

The ultimate goal of the Pond lab is to explore the mechanism by which HERG1A affects skeletal muscle atrophy. Here, our focus will be on identifying the source of increased $[Ca^{2+}]i$ and its downstream effects on protein degradation, specifically calpain enzymes and the calpain inhibitor calpastatin (i.e., their activity, abundance, etc.). We hypothesize that the increase in $[Ca^{2+}]i$ is not due to an increase in voltage gated calcium channels. Further, we hypothesize that calpain activity will increase as a result of the increase in $[Ca^{2+}]i$. Using an *in vitro* model, we have overexpressed *HERG1A* in C2C12 myotubes and produced a decrease in their area

thus simulating atrophy. We observed that in response to *HERG1A* overexpression, myotubes have an increase in voltage gated calcium channel 1.1 (Cav1.1) mRNA, however, at the protein level no difference was observed. This suggests that there is an increase in transcription but it is not being translated into a change in protein abundance – at least not a detectable change. Thus, it is not likely that the increase in calcium is a result of increased Cav1.1 channels. We have also been able to show an increase in calpain activity in response to 48 hour *HERG* transduction. The detected increase in calpain activity was shown not to be a result of an increase in transcription of calpains 1, 2, nor 3. Lastly, we investigated the amount of calpastatin present in response to HERG1A, results showed that calpastatin transcription is not affected by the presence of HERG1A. When immunoblots were performed no change in protein abundance was found in calpain 1. Interestingly, immunoblots for calpains 2 and 3 and calpastatin revealed that there was a statistically significant increase in their protein abundance (40.69%, 38.9%, and 37.7%, respectively).

CHAPTER 2

METHODS AND MATERIALS

Antibodies

Anti-Ca_v1.1 (extracellular) (Alomone labs, Jerusalem, Israel, Cat #: ACC-314)

Calpain-1 Polyclonal Antibody (BioVision, Milpitas, CA, Cat #: 3189-30T)

Calpain-2 Polyclonal Antibody (BioVision, Milpitas, CA, Cat #: 3372-30T)

Calpain-3 Polyclonal Antibody (ABclonal, Woburn, MA, Cat #: A11995)

Calpastatin Polyclonal Antibody (ABclonal, Woburn, MA, Cat #: A7634)

Cell Culture

C2C12 myoblasts were grown in Dulbecco's Modification of Eagle's Medium (DMEM) supplemented with 10% fetal bovine serum (FBS) and maintained in a humidified incubator with 10% CO_2 at 37ºC. To differentiate myoblasts into myotubes, cells were grown in DMEM supplemented with 10% FBS to ~85% confluence. The FBS medium was then removed from the cells and replaced with DMEM medium supplemented with 2% heat inactivated horse serum to initiate differentiation. Cells were incubated for 4 days in order to terminally differentiate into myotubes.

Collagen Coating of TC Plates

Due to an observed tendency for mature myotubes to release from the bottom of cell culture dishes, plates were treated with rat collagen prior to being seeded with cells. To coat the plates, 1mL of 1M acetic acid was added to 9mL of deionized water (or the

proportionate amount) and mixed to achieve a final concentration of 0.1M acetic acid. This solution was mixed with rat collagen to produce a final concentration of 1 mg/mL collagen. The plates were then coated with enough rat collagen solution to cover the bottom of the plate and these were then incubated for 1 hour at 37ºC. After an hour, the liquid was removed and the plates were washed with PBS twice. Plates were left under UV light overnight and then covered with parafilm and stored in the refrigerator until needed. When the plates were required they were incubated at 37ºC for 10 minutes before cells were plated.

Viral Transduction of Cells

At terminal differentiation (4 days post addition of horse serum medium), the myotubes were treated with 200 MOI virus (from a $2x10^{10}$pfu [plaque-forming units] stock suspension of viral particles) as was determined previously to produce HERG1A protein after 48 hours. The amount of virus needed was calculated by the equation:

$$X \cdot 200 = 2 \times 10^{10} pfu \cdot Y$$

Where X is the number of cells and Y is the amount of virus in milliliters which was then converted to microliters. One set of cells was treated with control GFP adeno-virus (VQAd EMPTY-eGFP; ViraQuest, New Liberty, IA) while the other received adeno-viral particles encoding the human ERG1A K^+ channel (VQAd CMV Herg-GFP; ViraQuest, New Liberty, IA). The amount of virus was then carefully pipetted into the correct volume of DMEM supplemented with 2% horse serum needed for the amount of plates/wells and triturated slowly. The HS medium that was present on the plates was drawn off with a pipet and replaced with the 2% HS medium treated with virus. The cells

were then incubated for 48 hours and monitored via fluorescence to verify that the transduction was successful.

RNA Isolation

For isolation of RNA cell cultures were rinsed with PBS followed by the addition of 0.5 mL cold Trizol reagent (Life Technologies; Carlsbad, CA) for one minute. Tissue culture plates (10 cm) with a confluent layer of C2C12 myotubes were then scraped with a clean lab spatula and this material was collected in a 1.5 mL Eppendorf tube. A 100 μL aliquot (20% of original volume) of chloroform was then added to the Eppendorf tube and this was vortexed for 30 seconds. The Eppendorf tubes were then centrifuged for 15 minutes at 12,000 rpm at 4°C. Following centrifugation, the top aqueous layer in the Eppendorf tube (~250 μL) was removed and placed into a clean 1.5 mL Eppendorf tube. A 250 μL aliquot of isopropanol was added to the aqueous solution, vortexed and incubated at room temperature for 10 minutes. The Eppendorf tubes were once again centrifuged for 10 minutes at 12,000 rpm at 4°C. The supernatant was decanted and 0.8 ml of 70% ethanol was pipetted onto the resultant pellet followed by centrifugation for 5 minutes at 12,000 rpm at 4°C. The supernatant was again decanted and the excess ethanol was carefully suctioned off and the pellet was allowed to air dry for 10 minutes. The pellet was then dissolved in 15 μL of DEPC treated water and incubated at 57°C for 10 minutes and finally vortexed briefly to precipitate all liquid. The RNA was then measured by UV spectrophotometry using a NanoDrop (NanoDrop ND-1000 spectrophotometer, Nanodrop Technologies, Thermo Fischer, Wilmington, DE).

DNase Digestion

The GOScript™ Reverse Transcription System Kit (Promega; Madison, WI) was used to degrade genomic DNA in the RNA samples using manufacturer's instructions and reagents provided in the kit. Briefly, a volume containing 3.5 μg of isolated RNA was brought to 8 μL with DEPC treated water. A 1 μL aliquot of 10X RQ1 Reaction buffer and 1 μL of RNase free DNase were added to the RNA and water. The reagents were then incubated in a thermocycler at 37°C for 30 minutes to degrade DNA and then the samples were incubated at 65°C for 10 minutes to denature the DNase enzyme. A 2 μL aliquot of 50 μM oligo(dT) was added to each sample and incubated at 70°C for 5 minutes, after which the samples were chilled on ice for 5 minutes. The sample tubes were then centrifuged lightly to collect the condensate.

cDNA synthesis

For the cDNA synthesis reaction, a reaction mixture was made with the following components per sample: 6 μL 5X GoScript RT buffer; 3.6 μL 25mM $MgCl_2$; 3 μL 0.1 M DTT;1 μL 10 mM dNTPs; 2.9 μL nuclease free water; and 1.5 μL GoScript reverse transcriptase. An aliquot of this reaction mixture (18 μL) was placed into an appropriate RNase- and DNase-free microtube along with 2 μL of each sample. Samples were placed in a thermocycler to incubate at 25°C for 5 minutes, 42°C for 1 hour, and 70°C for 15 minutes. Once synthesis was complete, the cDNA samples were stored at -20°C (final volume = 30 μL).

Primer Design

Primers were designed using the NCBI Primer – BLAST program and DNA sequences downloaded from NCBI except where noted. The criteria used to design primers were as follows: amplicon length of 50 – 210 base pairs, primer length of 18 – 23 nucleotides, a GC content of 35 – 65%, and a melting temperature between 57 – 67°C. The following sequences were used (Table 1). All primers were obtained from Integrated DNA Technologies (Coralville, IA).

Table 1. Sequences of RT-PCR primers.

Primer Name (mouse)	Primer Sequence 5' – 3'	Size (bp)	Tm (°C)	GC (%)	Amplicon Size (bp)
Merg1a Forward	cctcgacaccatcatccgca	20	59.6	55.0	145
Merg1a Reverse	aggaaatcgcaggtgcaggg	20	60.3	60.0	
18S Subunit Forward	cgccgctagaggtgaaattct	21	57.2	52.4	101
18S Subunit Reverse	agaacgaaagtcggaggttc	20	57.0	52.4	
Cav1.1 Forward	gtcccaccaacaagatccgt	20	57.3	55.0	88
Cav1.1 Reverse	gctgagcaggatgaagagca	20	57.4	55.0	
Cav1.1e Forward**	ctaatcgtcatcggcagcat	20	55.1	50.0	59
Cav1.1 embryo Reverse**	tctcatctgggtcatcgatct	21	54.8	47.6	
Cav1.2 Forward*	atgcaagacgctatgggctat	21	56.5	47.6	201
Cav1.2 Reverse*	caggtagcctttgagatcttcttc	24	55.0	45.8	

Cav1.3 Forward	gctggacatgctggttgttg	24	55.2	41.7	116
Cav1.3 Reverse	ttgattgctctgagaggccg	22	56.5	50.0	
Calpain 1 Forward	gctaccgtttgtctagcgtc	20	58.73	55.0	98
Calpain 1 Reverse	taactcctctgtcatcctctggt	23	59.99	47.83	
Calpain 2 Forward	ttttgtgcggtgtttggtcc	20	59.83	50.0	107
Calpain 2 Reverse	aactcagccacgaagcaagg	20	60.89	55.0	
Calpain 3 Forward	ttcacaggaggggtgacaga	20	60.11	55.0	122
Calpain 3 Reverse	ttcgtgccatcgtcaatggag	21	61.01	52.38	
Calpastatin Forward	gccttggatgacctgataga	20	53.8	50.0	115
Calpastatin Reverse	gtgcctcaaggtaggtagaa	20	53.7	50.0	

*Primer sequence was obtained from B.Schlick et. al. [33].

**Primer Sequence was obtained from Nasreen Sultana et. al. [34].

Primer Efficiency Determination

To determine the efficiency of the primer sets, a standard curve was generated using dilutions (e.g., 1:2, 1:4, 1:8, 1:16, and 1:32) of an appropriate standard (known plasmid or cDNA from a known tissue sample, such as heart for Cav1.2 and adrenal glands for Cav1.3), which were assayed by real time PCR using a C1000 Thermocycler machine (BioRad; Hercules, CA). Standards were assayed in triplicate and then standard Ct was plotted against the log of the standard concentration. Using Microsoft Excel (Excel 2013, Microsoft, Redmond, WA), the linearity was calculated using the R-square method and the slope of the line was determined and used to calculate the efficiency of the primers: $10^{(-1/\text{slope})}$. Percentage determination was done by: $\frac{\text{efficiency}}{2} \times 100$. The primer efficiency was considered acceptable at 95 – 105% with R-square values of 0.985 or above for the standard curve.

Quantitative Real Time PCR (qRT-PCR)

Primer stocks for quantitative real time PCR were diluted with nuclease free water so the final concentration of each primer was 100 μM. Primers were then diluted 1:5 to a final volume of 100 μl (20 μM), making a working solution. Master mixes were made so that 18 μl of this mix would contain: 7 μl of autoclaved water, 1 μl of primer mix (forward and reverse primers diluted in autoclaved water) final concentration of 1 μM, and 10 μl of SYBR green. A master mix was made which contained primers for the gene of interest and a second master mix was made which contained primers for a “house-keeping” gene for normalization. An 18 μl aliquot of the each master mix was loaded into wells of a 96 well plate (Thermo Scientific, Waltham, MA) in triplicate and a 2 μl

aliquot of each cDNA sample was added to the triplicate wells, with the exception of a single triplicate set of wells which received a 2 μL aliquot of non-template control (i.e., a sample which had undergone all steps of the process without any RNA) per master mix. An Applied Biosystems 7300 Real Time PCR machine was used for all qPCR work with *HERG*/*Merg* to determine Ct values (Applied Biosystems; Foster City, CA). For all other qPCR data a BioRad CFX96 Real Time System was used to determine Ct values (BioRad; Hercules, CA). To normalize the data, the average Ct values for the target gene were compared to that of the house-keeping18S rRNA (18S). The average Ct of each triplicate was taken for both the target gene and the reference 18S gene. The fold change was then determined via the $2^{-\Delta\Delta Ct}$ (Livak) method (Bio Rad Laboratories, Real-Time PCR Applications Guide, 2006) and an average Ct of each triplicate first taken (Ct).

Ct(target) – Ct(ref) = ΔCt, ΔCt - $\Delta Ct_{(con,\ 0\ hr)}$ = $\Delta\Delta$Ct, $2^{-\Delta\Delta Ct}$ = normalized expression ratio.

Protein Harvest

Medium was aspirated and the plates were then rinsed gently with 30-37ºC PBS three times. A 0.3 ml aliquot of 10mM Tris 1mM EDTA (TE) containing 2% Triton X-100 and protease inhibitors (listed below) were then rinsed over each plate surface with an Eppendorf tip or pipetteman while scraping the surface with the pipette tip. Plates were then scraped with rubber policeman or a Teflon stirrer. Cells and cell debris were aliquoted into an Eppendorf centrifuge tube and placed on ice. A 0.2 ml aliquot of TE buffer was added to the plate and scraped over the surface as before. The solid material was scraped into the liquid and pipetted into the Eppendorf tube and pooled

with the earlier aliquot. The sample was then triturated with a tuberculin syringe and 23G1 needle until solid particles were broken up. The tubes were then left on ice and placed in the refrigerator for 30 minutes to solubilize. It was then triturated a second time with a syringe and needle for 1-2 minutes. Eppendorf tubes with material were then centrifuged in a tabletop centrifuge for 2 minutes at 15,000 rpm. If the supernatant appeared cloudy or large amounts of solid were present the supernatant was removed to a second Eppendorf tube and centrifuged a second time. The aliquot was then frozen, retaining a small amount (~20μl) for protein microassay.

Protease inhibitors per 100ml of TE buffer:

500μl of 100mM stock pefabloc or PMSF (in ethanol) (final = 0.5mM)

100μl of 1mM (0.7 mg/ml) stock pepstatin (final = 1mM)

2.0ml of 50mM stock benzamidine (final = 1mM)

200μl of 2.0mg/ml stock aprotinin (final = 4μg/ml)

1.0ml of 100mM stock Iodoacetamide (final = 1mM)

1.0ml of 100mM stock 1,10-phenanthroline (final = 1mM)

Protein Microassay

Protein assays were done using a DC Protein assay kit (BioRad, Hercules, CA) using the microplate assay protocol. Working reagent was made up using 20μl of reagent S added to every ml of reagent A needed (A'). Protein standards were made using bovine albumin at concentrations of 0.25mg/ml to 2mg/ml in order to prepare a

standard curve. A 5μl aliquot of both standards and samples were pipetted into the wells of a 96-well microtiter plate. Then 25μl of reagent A' was added to each well followed by 200μl of reagent B. The plate was gently mixed and allowed to sit at room temperature for 15 minutes. Absorbances were then read at 750nm using a Synergy H1 Hybrid Reader (BioTek Instruments, Winooski, VT).

Western Blot

Polyacrylamide SDS gels (separating gel 7.5% and stacking gel 4% acrylamide) were poured. BioRad Kaleidoscope Precision Plus Protein Standards (BioRad, Hercules, CA; 12μl) were used with each electrophoresis run. Sample protein (protein amounts as indicated in each figure, 20μl) were combined with 5μL of 5X sample diluting buffer (0.3M Tris, 50% glycerol, 5% SDS, 0.5M DTT, and 0.2% Bromophenol Blue) and boiled in water for five minutes. The gel was then loaded with standard and samples and electrophoresed at 200V until the dye front exited the gel. The proteins were then transferred to PVDF transfer membrane (BioRad, Hercules, CA 0.2μM pore size). Specifically, the membrane was initially soaked in methanol, rinsed in deionized water, and then placed in transfer buffer (10% 10X electrode buffer, 20% methanol, and deionized water). Once electrophoresis was complete, the gel was removed and placed on the aforementioned membrane and filter papers and placed in a transfer apparatus (Trans-Blot® Cell; BioRad) filled with transfer buffer. A current was run through at 400mAmps for an hour and a half. The gel was carefully removed and excess membrane was cut away and the lanes were cut out and separated according to the antibody into which each would be incubated. The membrane was rinsed in PBS 3

times for five minutes each rinse. The sample containing membrane was then incubated in a blocking buffer (0.2% I-Block (Applied Biosystems; Foster City, CA), 0.1% Tween-20 in 1X PBS, pH 7.4) and placed on a rocker for one hour. The necessary primary antibody was diluted (per figure legends) in a second blocking buffer (5% NGS, 0.2% Triton X-100, 0.1% sodium azide in PBS) and the primary antibody was placed on top of the membrane and left in the refrigerator in a wet chamber overnight. The next day the membranes were removed from primary antibody and were rocked for 10 minutes each in two changes of I-block buffer (0.2% I-Block, 0.1% Tween-20, 1X PBS). It was then removed from the buffer and incubated in a goat anti-rabbit alkaline phosphatase (AP)-conjugated secondary antibody (diluted 1:1000 in I-block buffer) for 1 hour. The secondary antibody was removed and the membranes were washed three times for 15 minutes in I-block buffer. The membrane was then washed twice in assay buffer (0.1% Tween 20 in TBS). Membranes were then laid down on a plastic block and Immun-Star AP substrate (BioRad, Hercules, CA) at 37ºC was applied to the membranes for five minutes. The substrate solution was then removed and the membranes were blotted with Kim Wipes before being wrapped in clear plastic wrap. These were taken to a dark room and developed using a SRX-101A film processor (Konica Minolta, Chiyoda, Tokyo, Japan). After films were developed, they were scanned into a computer and ImageJ was used to measure optical densities of each band.

Calpain-Glo Assay

Myotubes were differentiated for four days in horse serum media in 24 well plates followed by transduction with 200MOI HERG1A or GFP virus (12 wells each). Wells were then washed with two changes of 37°C PBS. A Calpain-Glo™ Protease Assay kit

(Promega, Madison, WI) was used to assay calpain activity. The kit included a Calpain-Glo Buffer, Suc-LLVY-Glo Calpain Substrate, and Luciferin Detection Reagent which, when combined, is referred to as Calpain-Glo Reagent. A stock buffer solution of 0.2% Triton X-100 in PBS and 200nM epoxomicin (BostonBiochem, Cambridge, MA, Cat. #I-110) was made in order to permeabilize the cells (Triton) and inhibit the proteasome (epoxomicin). To begin, 200µl of the 4 separate buffer solutions each containing either 2.0mM EDTA, 2.0mM $CaCl_2$, or buffer alone were added to 6 wells (3 Control, 3 HERG). These were allowed to sit at room temperature for 5 minutes to ensure the cells were permeabilized and the proteasome inhibited. After 5 minutes 200µl of the Calpain-Glo reagent was added to all wells and allowed to sit at room temperature for 15 minutes. A 200µl aliquot of the liquid was removed to a white-walled 96 well plate and luminescence was read by a Synergy H1 Hybrid Reader (BioTek Instruments, Winooski, VT). The remaining well contents were scraped from the back of the plate, triturated using a syringe and 26 gauge needle and then centrifuged to remove solid material. The supernate was assayed for protein content using the BioRad DC kit (described above). The protein data were used to normalize the calpain activity.

Statistics

In general, statistics were done using a simple student t-test and SAS (SAS Inc.; Carey, NC). Results were considered significant when $p<0.05$.

CHAPTER 3

RESULTS

Specific Aim I: An in *vitro* model of HERG1A Overexpression in C2C12 myotubes.

ERG1 Protein Content in Myoblasts and Myotubes. To study the effect of HERG1A expression on myotubes, we first had to develop an *in vitro* model overexpressing *HERG1A*. This first entailed determining the amount of native MERG1A protein detectable in both C2C12 myoblasts and 5 day differentiated myotubes. Western blot revealed a statistically significant 40.7% greater abundance of MERG1A protein in myotubes than in myoblasts ($p<0.01$; Figure 8).

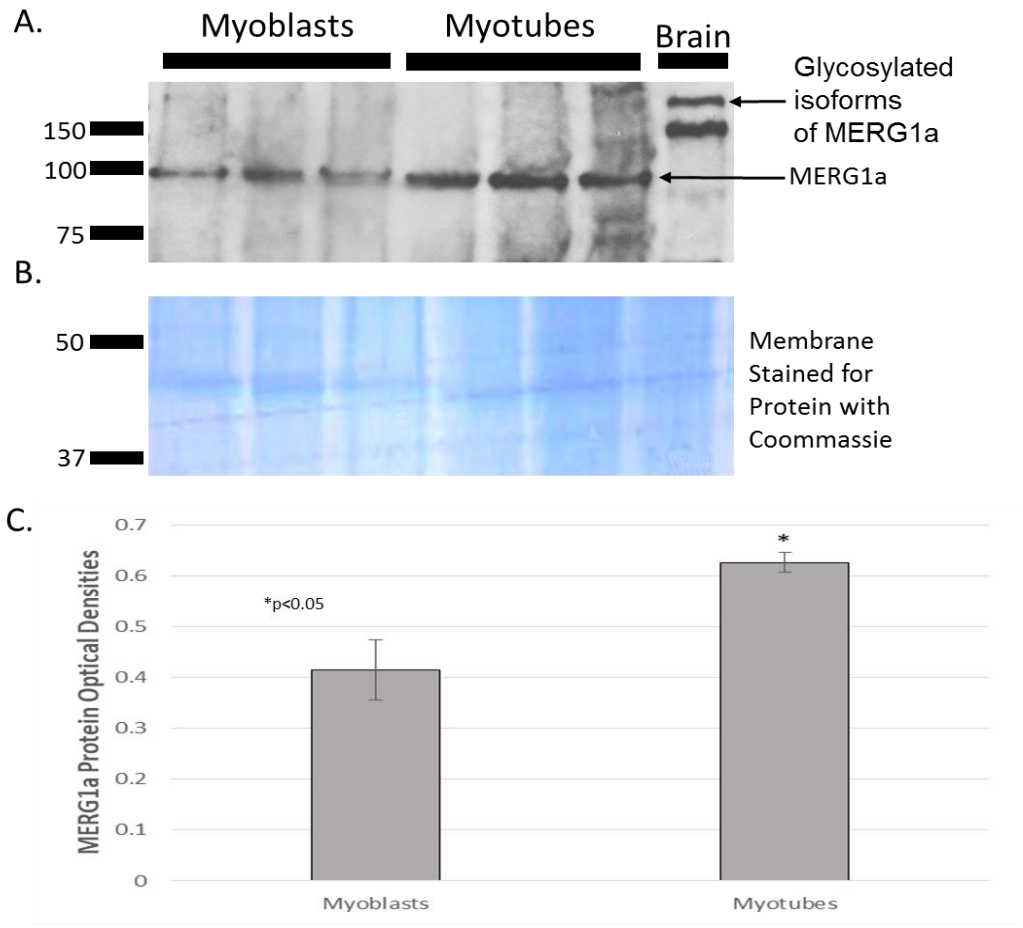

Figure 8. Expression of MERG1A protein is 40.7% higher in myotubes than in myoblasts. **(A)** Western blot shows protein levels of MERG1A in undifferentiated myoblasts and myotubes (50μg protein per lane). Protein extracted from mouse brain was used as a positive control. **(B)** To show that equal amounts of protein were loaded into each lane, the membrane was stained for protein with Coomassie blue (G-250; BioRad, Hercules, CA). **(C)** The mean optical densities from three samples are shown here with a bar graph. The bars represent the mean of three samples while with the error bars revealing the standard error of the mean (mean ± SEM).

Overexpression of HERG1A in Myotubes. We next wanted to determine to what extent the HERG1A protein would be overexpressed in response to the transduction of myotubes with HERG1A virus. Thus, the HERG1A and control adenoviral particles, both encoding GFP, were transduced into myotubes. The HERG1A treated myotubes were found to have an increased amount of HERG1A protein while, as expected, the control myotubes showed no HERG1A protein present. Optical densities were determined, revealing that there was no difference in MERG1A protein levels between control and HERG1A-transfected cells (Figure 9).

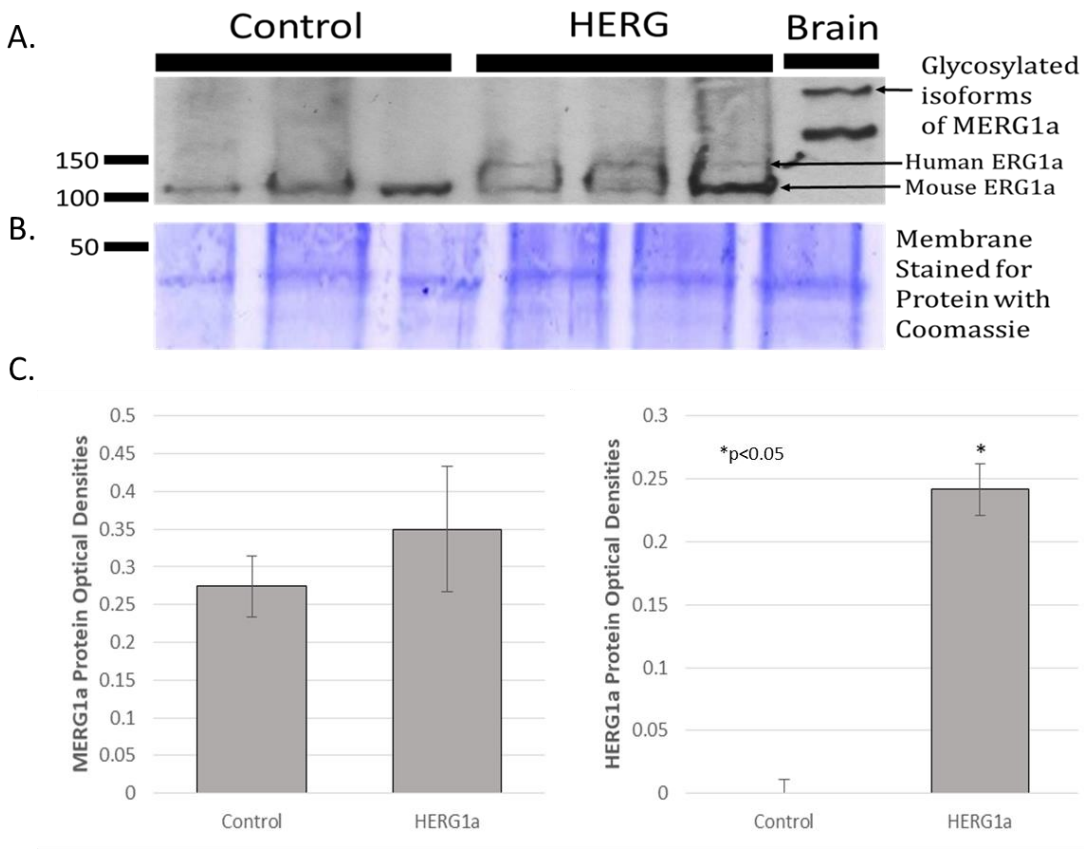

Figure 9. HERG1A can be overexpressed in myotubes using viral particles. **(A)** HERG1A and MERG1A protein (50μg protein each lane) are detected in C2C12 myotubes 48 hours after transduction with HERG1A virus whereas control cells solely express MERG1A. Protein extracted from mouse brain was used as a positive control and **(B)** the membrane was stained for protein using Coomassie blue stain to demonstrate that equal amounts of protein were loaded into each well. **(C)** The mean optical densities from three experiments were plotted as a bar graph. The bars represented the mean and error bars represented the standard error of the mean (mean ± SEM).

Overexpression of HERG1A Induces Atrophy in Myotubes. To explore further the effect of the HERG1A channel on muscle, we transduced myotubes with control and HERG1A-encoded virus and imaged the cells at 48 and 72 hours post-treatment (Figure 10A). We measured the area of the myotubes and discovered that HERG1A treatment produced a significant 30.5% and 21.4% decrease in myotube area at 48 and 72 hours post transduction, respectively ($p<0.01$) (Figure 10B). At this point, we have ensured that our viral transduction is successful in penetrating the cell, translating the encoded protein, and decreasing the size of the cell, thus simulating atrophy *in vitro*.

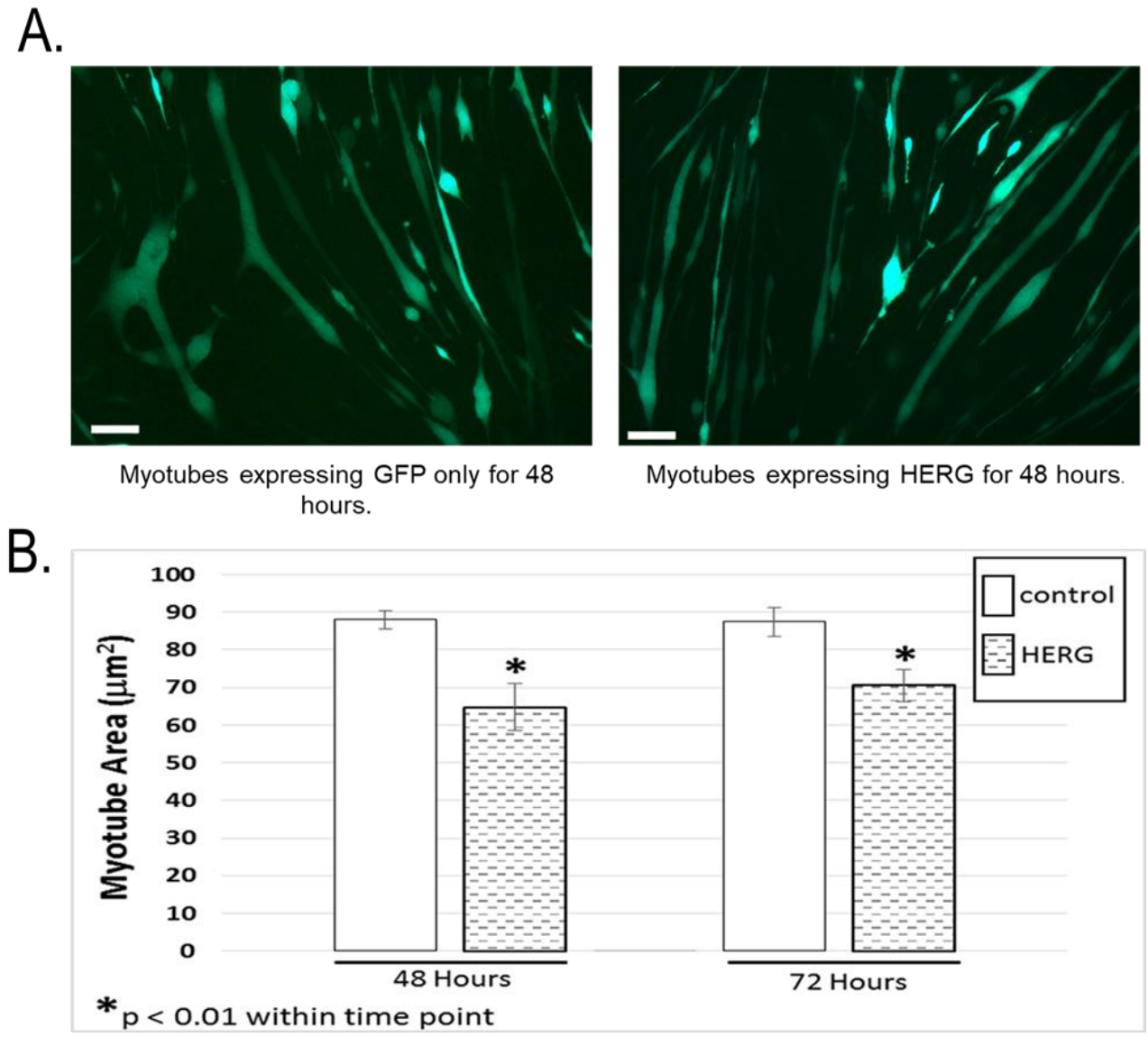

Figure 10. HERG1A expression in C2C12 myotubes induces a decrease in myotube area. **(A)** Images of control and HERG expressing myotubes at 48 hours post transduction. Scale bar = 50 □m. **(B)** Myotube area was determined using ImageJ and revealed a significant 30.5% decrease in cell size when cells were treated with HERG1A. Bars representthe mean of three experiments with the standard error of the mean (mean ± SEM) represented by error bars (left to right n= 69, 63, 81, 78).

Our results have allowed us to demonstrate that we have a successful *in vitro* model of skeletal muscle atrophy resulting from over-expression of the voltage gated potassium channel *HERG1A* in C2C12 myotubes. Differentiated myotubes presented with a greater abundance of MERG1A protein than the undifferentiated myoblasts. Transduction with an adenovirus coding for *HERG1A* was shown to successfully synthesize the HERG1A protein within myotubes and cause a decrease in myotube area. This data combined allowed us to conclude that we have successfully simulated atrophy using a *HERG1A* encoded adenovirus in C2C12 myotubes.

Specific Aim 2: Investigation of the effect of HERG1A on voltage gated calcium channels.

Observation of the increase in intracellular calcium resulting from HERG1A overexpression (Figure 7) led us to question the source of this increased calcium. We wanted to determine if the calcium was coming from the exterior through sarcolemmal L-type calcium channels or was it perhaps released from internal stores of calcium. Because the ERG1A channel is detected in the sarcolemmal membrane, where the Cav1.1 calcium channels are found in skeletal muscle, we turned our attention to the voltage gated calcium channel family (i.e., CAV, DHPR), specifically Cav1.1, 1.2, and 1.3, and included the Cav1.1e splice variant found only in the embryonic stage.

HERG1A Overexpression Does Not Affect Expression of Cav1.2 and 1.3. Cav1.1 mRNA levels were not significantly different from controls at 48 hours after transduction (Figure 11A) which is when we detected an increase in intracellular calcium concentration (Figure 7). The embryonic splice variant, Cav1.1e, was also examined, however, no difference in that mRNA level in response to HERG1A was detected (Figure 11B). Interestingly, we did detect a significant 2.26 fold increase in Cav1.1 mRNA at 72 hours after transduction with the HERG1A virus (Figure 11A); however, the increase in intracellular calcium concentration was detected prior to this time point. As expected Cav1.2 and 1.3 were not expressed in the skeletal muscle of mice nor in the C2C12 cells even after treatment with *HERG1A* (data not shown).

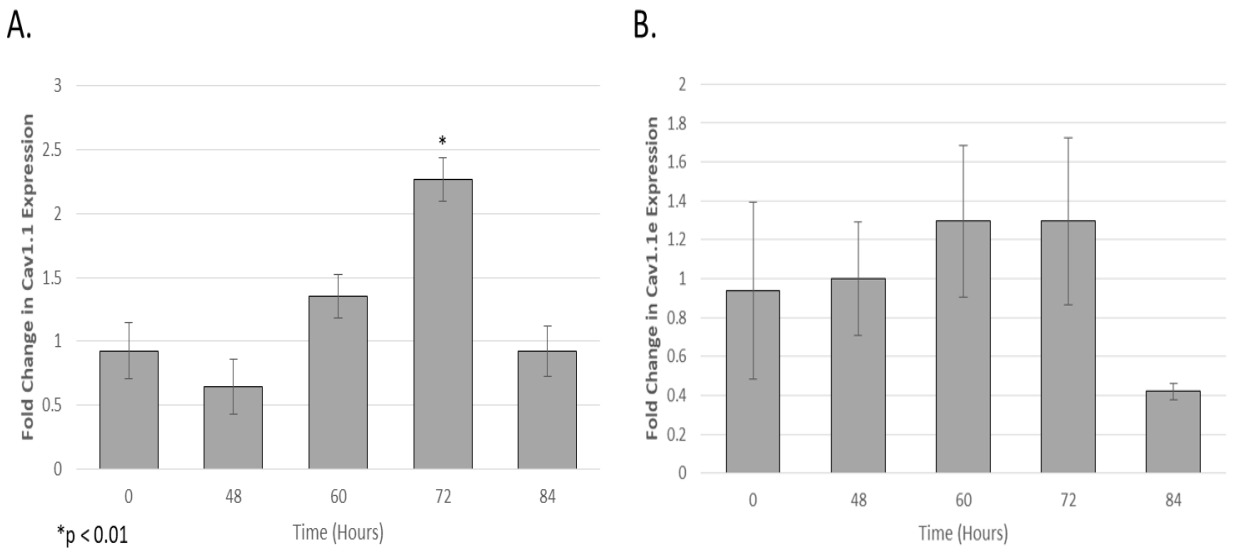

Figure 11. Cav1.1 channel mRNA increases in HERG1A treated myotubes at 72 hours after transduction. **(A)** Expression of HERG1A in C2C12 myotubes shows a significant 2.3 fold increase in voltage gated calcium channel 1.1 (*Cav1.1*) gene expression 72 hours post transduction, although there is no significant increase at 48 hours post transduction when the increase in intracellular calcium concentration is noted. **(B)** There was no significant difference in the amount of gene expression of the embryonic voltage gated calcium channel (*Cav1.1e*). Gene expression was compared to that of an *18S* positive control. Bars represent means while error bars represent the standard error of the mean (mean ± SEM; n=3).

In order to support the real time PCR data, an immunoblot was performed on C2C12 myotubes that were treated with either control or HERG1A virus (Figure 12). The cells were transduced for 96 hours. Note: This time point is 24 hours past the time point at which we saw the increase in mRNA which would allow enough time for transcription and translation of the voltage gated calcium channel to take place. Our

results show that there was no change in the abundance of protein in the myotubes at this time, although we saw an increase of mRNA expression through qPCR. We suspect that the small increase in Cav1.1 transcription detected by qPCR is either not physiologically significant enough to produce an increase in translation and thus protein abundance or the difference in protein abundance is not detectable.

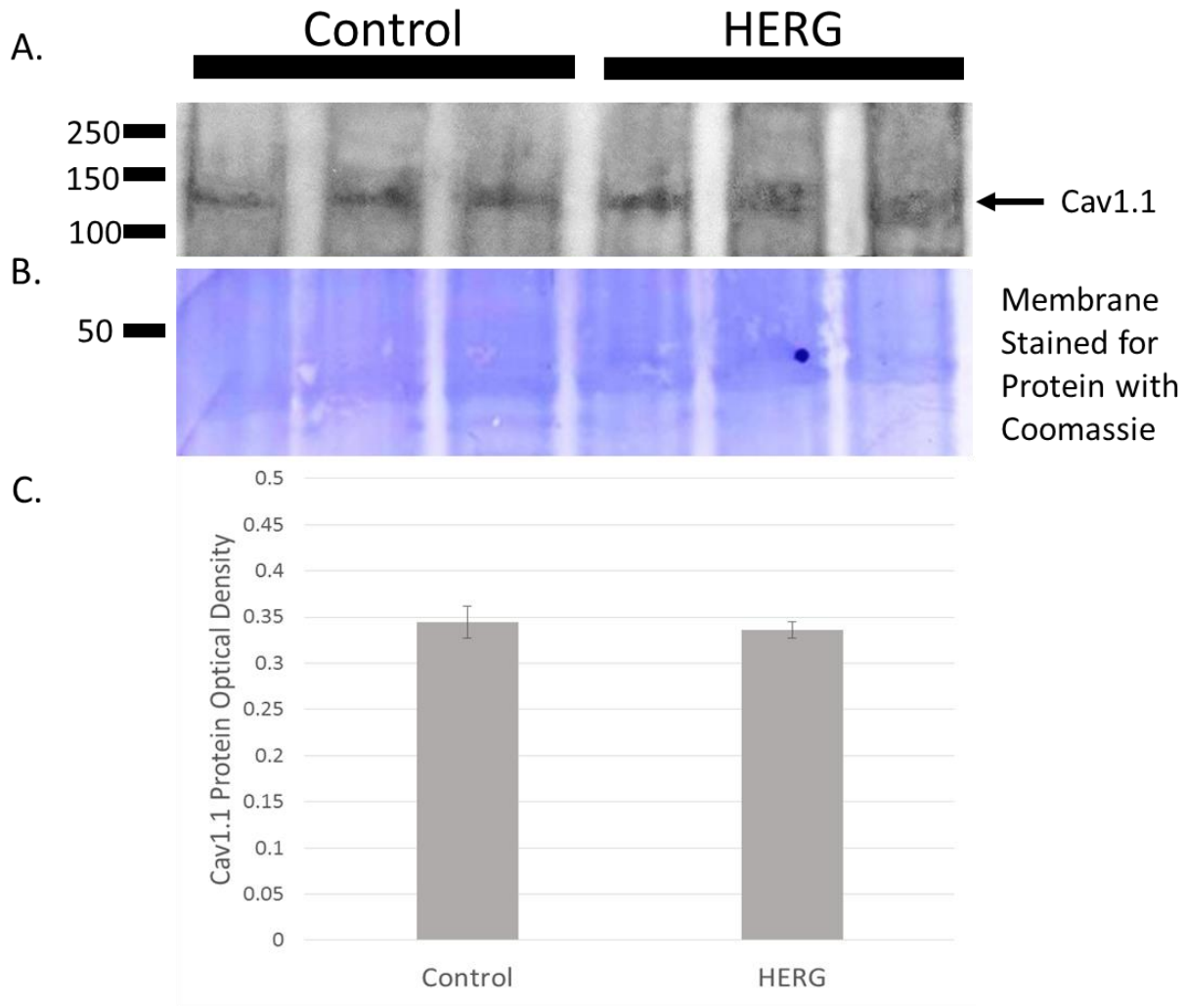

Figure 12. Cav1.1 protein abundance did not change in response to HERG1A expression in C2C12 myotubes**. (A)** Immunoblot for the L-type voltage gated calcium channel Cav1.1 (65μg protein per lane). **(B)** Coomassie blue stain of the PVDF membrane for protein shows that equal amounts of protein were added to each lane. **(C)** No significant difference in the amount of protein was detected in HERG1A treated cells compared to those of the control cells at 96 hours after transduction with the HERG1A virus. Bars represent means while error bars represent the standard error of the mean.

Specific Aim 3: Investigation of the effects of HERG1A-modulations of calpain activity.

Because HERG1A transduction results in increased intracellular calcium concentrations (Figure 7; [32]), we next wanted to investigate the downstream effects of this increase. Specifically, we began by monitoring activity of the calcium-activated calpain enzymes. Cells were treated with 1mM final concentration of calcium to ensure that calpain activity could be measured and 1mM EDTA, a calcium chelating agent, was used to remove calcium from the system to yield a baseline level of non-calcium activated proteolytic activity. We used a Calpain-Glo assay kit (ProMega; Madison, WI) to monitor the combined activities of both calpain 1 and 2 and observed a 25.7% increase in basal calpain activity at 48 hours after transduction with HERG1A encoded viral particles (Figure 13).

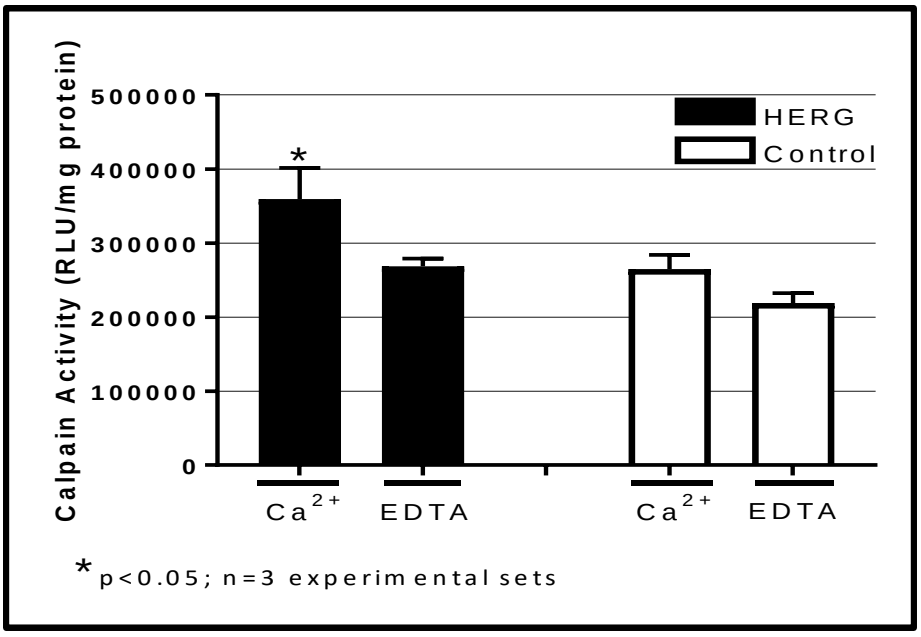

Figure 13. Calpain activity was increased by a significant 25.7% in HERG1A treated C2C12 myotubes. The calpain activity in the calcium treated control cells was 19.2% greater than that in the EDTA treated control cells, but the difference was not statistically significant. Bars represent means and error bars represent standard error from the mean (mean ± SEM; n=3).

Calpain enzymes are calcium activated and thus the activity will increase with increased intracellular calcium. However, we cannot assume that the increased calcium is the only explanation for the increased calpain activity. Other possible causes include: increases in calpain transcription and/or calpain protein levels or a decrease in calpastatin (a conventional native calpain inhibitor) transcription and/or its protein levels. Thus, we asked if calpain and calpastatin transcription levels (i.e., amount of mRNA produced) changed in response to HERG1A treatment. We used quantitative real time PCR and revealed that, although HERG1A treatment may produce a potential small trend of calpain 2 increase over time for 72 hours post viral transduction, it does not

produce a statistically significant change in calpain 2 gene expression for 84 hours after viral treatment (Figure 14). Further, no change in gene expression was detected for calpains 1 or 3 (data not shown).

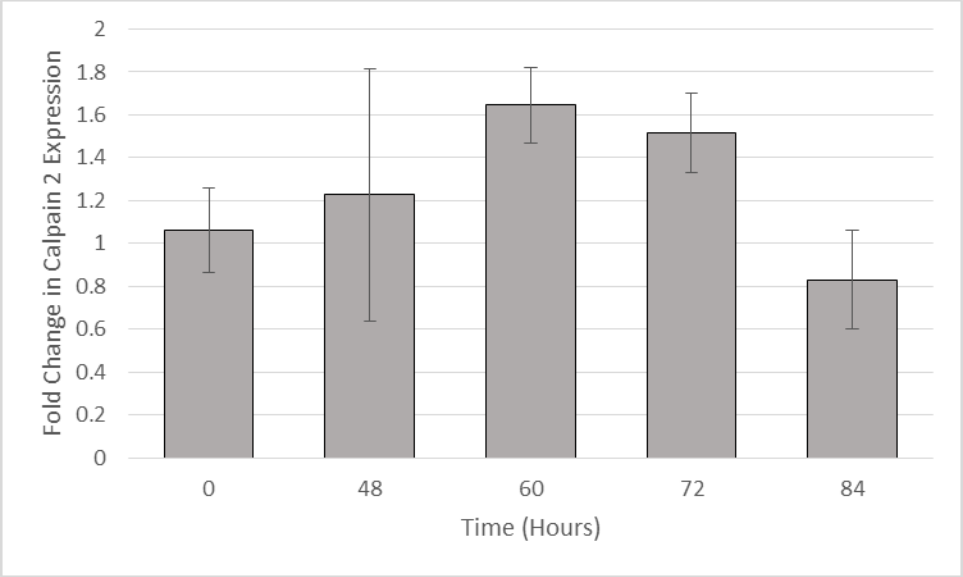

Figure 14. Expression of HERG1A in C2C12 myotubes did not produce a significant difference in calpain 2 gene expression. Bars represent means and error bars represent standard error from mean (mean ± SEM; n=3).

Immunoblots were performed to determine if there was any change in the amount of calpastatin or specific calpain protein in response to HERG1A treatment. For calpain 1, the optical densities of both bands in the doublet were measured and the statistics performed show that there is no difference in calpain 1 protein abundance (Figure 15).

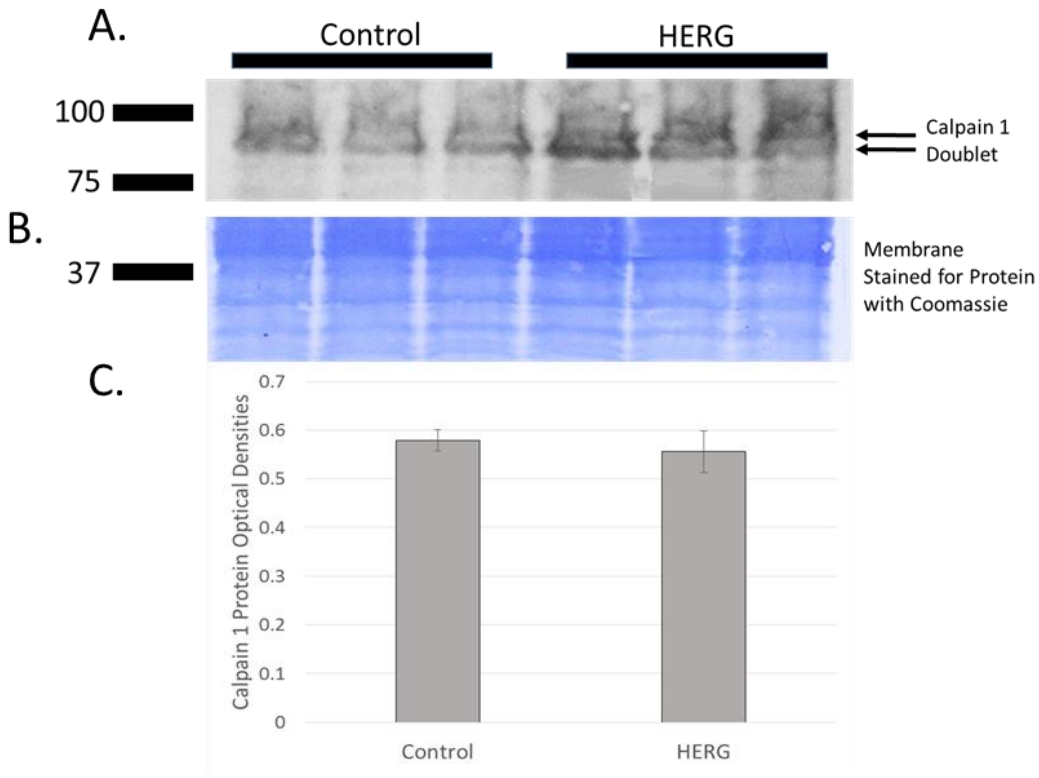

Figure 15. Calpain 1 protein abundance was not affected by HERG1A treatment. **(A)** Immunoblot of myotube lysates for calpain 1 (60μg) reveals that there is no significant difference in the amount of calpain 1 protein in HERG1A treated myotubes compared to those of the control at 48 hours after transduction. **(B)** Coomassie blue stain of PVDF membrane proteins shows that equal amounts of protein were loaded into each lane. **(C)** HERG1A treatment of myotubes did not affect significantly affect calpain 1 protein abundance. The bars represent the means while error bars representing the standard error of the mean (mean ± SEM; n=3).

Calpain 2, when autolyzed and hence activated, has been seen to appear as two separate bands as stated previously. Figure 16 demonstrates this doublet found at ~75Kd. Our results show that there is in fact a 40.69% decrease in calpain 2 (i.e., m-

calpain) in response to HERG1A treatment.

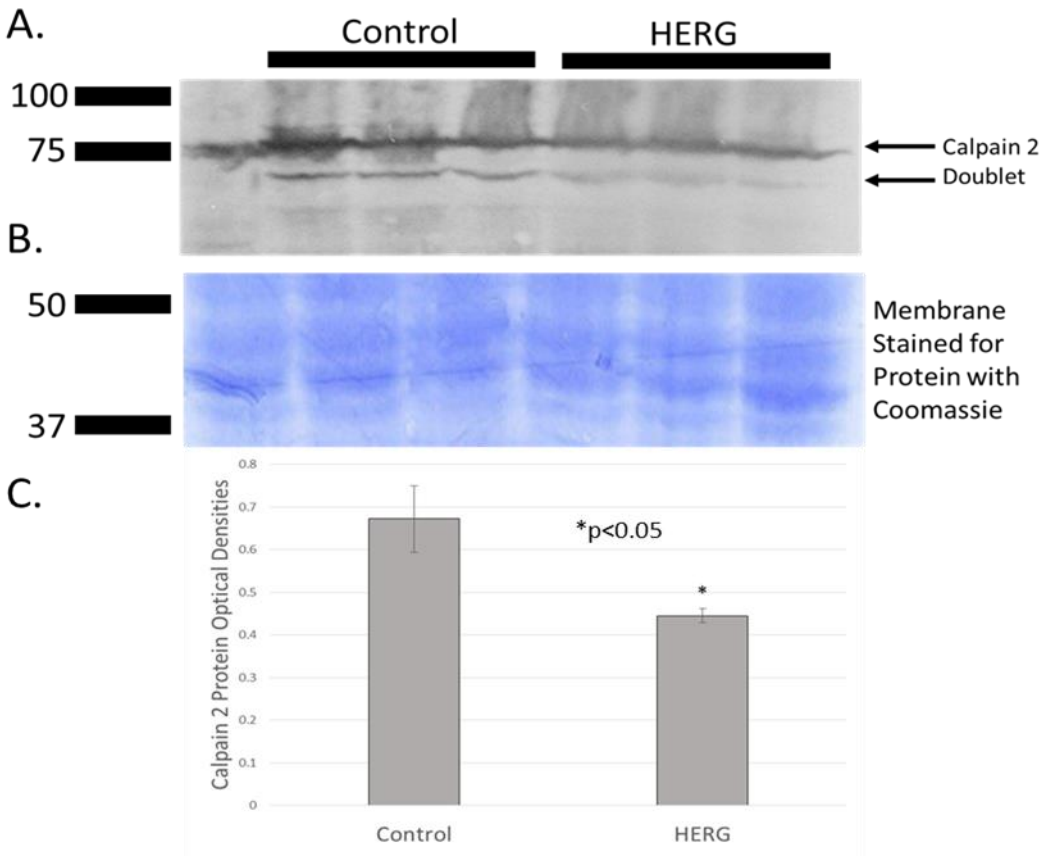

Figure 16. There is a 40.69% decrease in calpain 2 protein abundance in HERG1A transduced myotubes. (**A**) Immunoblot for calpain 2 protein (60μg per lane). (**B**) To show that equal amounts of protein were loaded into each lane, the membrane was stained for protein with Coomassie blue. (**C**) HERG treatment resulted in decreased calpain 2 protein abundance. Bars represent the mean of three samples while error bars represent the standard error from the mean (mean ± SEM; n=3).

Calpain 3 is a skeletal muscle specific calpain that is not calcium dependent and, like other calpains, is believed to take part in the degradation of anchoring proteins. However, it is also suggested that calpain 3 takes part in the remodeling of the

sarcomere in times of cellular stress. We immunoblotted for calpain 3 protein and discovered that there is indeed a significant 38.9% decrease in calpain 3 protein abundance in response to HERG1A treatment (Figure 17).

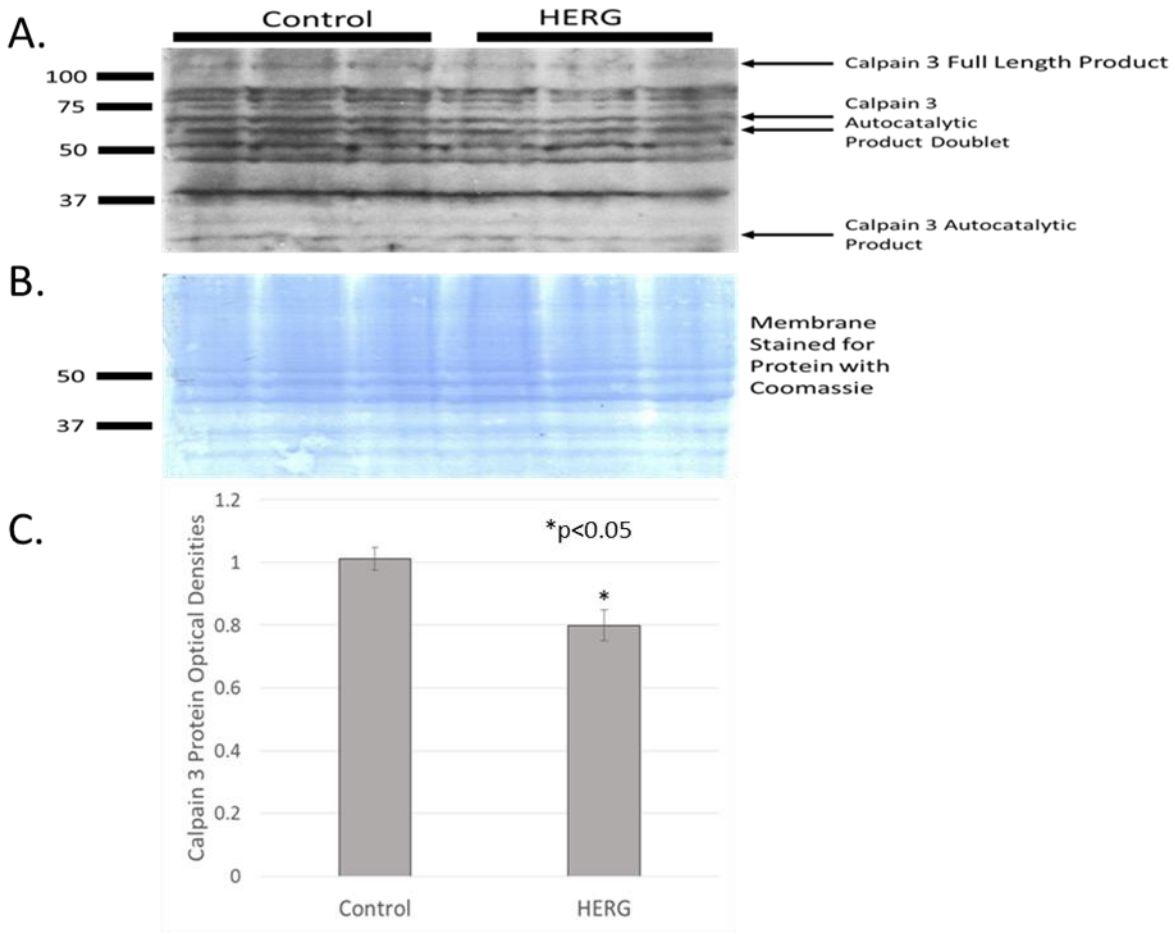

Figure 17. There is a significant 38.9% reduction of calpain 3 protein in C2C12 myotubes in response to HERG1A expression. A. Immunoblot of calpain 3 (60μg protein per lane). B. Coomassie blue protein stain of transferred PVDF membrane demonstrates that equal amounts of protein were added to each well. C. A significant 23.48% reduction of calpain 3 protein was observed. Bars represent the mean of three samples with error bars representing the standard error from the mean (mean ± SEM; n=3).

Calpastatin, as previously, stated is a native inhibitor of conventional calpains. Therefore, we were interested in investigating the effect of HERG1A treatment on calpastatin transcription and protein levels. Again using C2C12 myotubes and quantitative real time PCR, we measured the amount of calpastatin mRNA present in response to HERG1A treatment. Our findings revealed that there was no significant change in calpastatin mRNA in response to HERG1A treatment over 84 hours. (Figure 18).

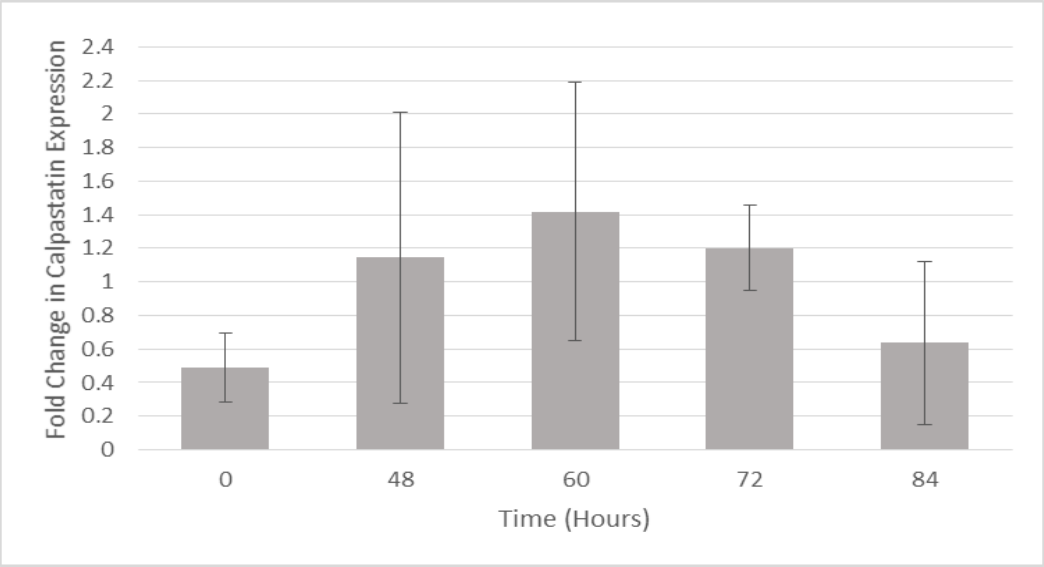

Figure 18. Quantitative PCR shows that there was no significant change in calpastatin gene expression in response to HERG1A expression. The fold change in calpastatin mRNA showed no significant difference when compared to the 18S reference gene. Bars represent the mean and error bars represent the standard error of the mean (mean ± SEM; n=3).

Immunoblots were done to observe the amount of calpastatin protein. The results show that there is a significant 37.7% decrease in calpastatin abundance found in the HERG1A transduced cells as opposed to control cells (Figure 19).

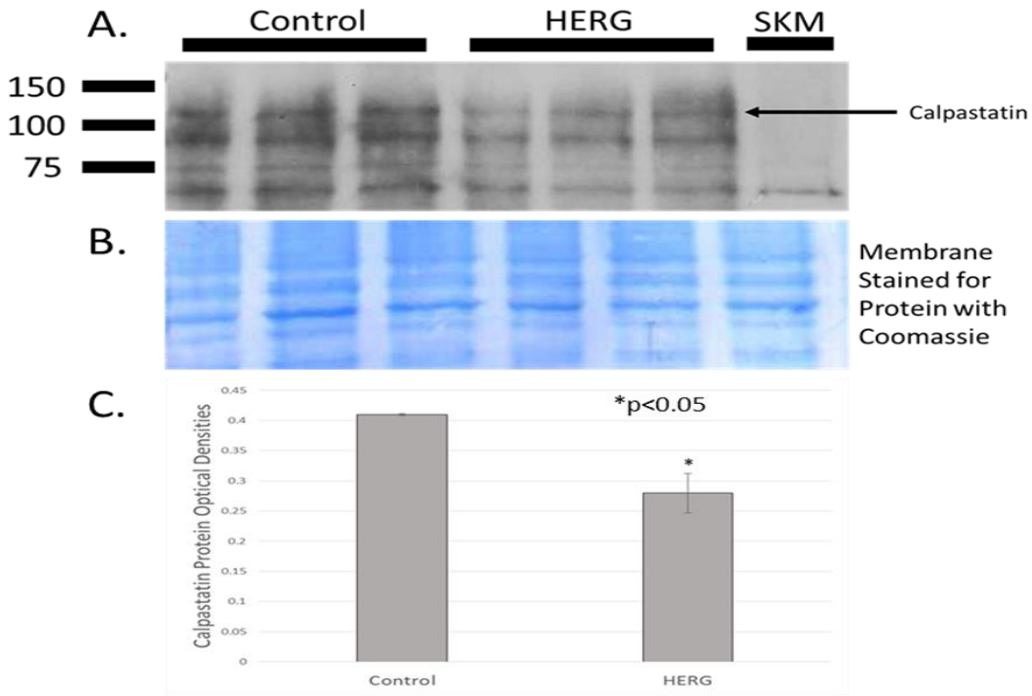

Figure 19. Calpastatin protein abundance was decreased by a significant 37.72% in myotubes treated with HERG1A. A. Immunoblot of control and HERG1A treated myotubes (60μg protein per lane). B. Coomassie blue protein stain of transferred PVDF membrane demonstrates that equal amounts of protein were added to each well. C. Calpastatin protein abundance decreases in response to HERG1A. Bars represent the mean of three samples while error bars represent the standard error from the mean (mean ± SEM; n=3).

CHAPTER 4

DISCUSSION

The ERG1a voltage-gated K^+ channel is responsible for late repolarization of the cardiac action potential and was thought to be absent from skeletal muscle [23, 35], however, the Pond and Hannon labs demonstrated that this protein is detectable in atrophying skeletal muscle [24]. Consequent studies have shown that ERG1a expression leads to an increase in the E3 ubiquitin ligase MURF1 and contributes to activation of the ubiquitin proteasome proteolysis known to contribute to skeletal muscle atrophy [24, 25]. A new study has now shown that ERG1a expression also increases the amount of $[Ca^{2+}]i$ in C2C12 myotubes (unpublished data, Pratt, Hockerman, Pond 2018) (Figure 6). However, the source and downstream effects of the calcium increase have yet to be investigated. Here we have initiated these studies.

We have shown that HERG1A increases intracellular calcium in C2C12 myotubes. There are numerous mechanisms by which this could occur. For example the IP_3 pathway, in which a G coupled receptor (GPCR) activates phospholipase C (PLC), which in turn cleaves phosphatidylinositol 4, 5 bisphosphate (PIP_2) into IP_3 and diacylglycerol (DAG). The IP_3 binds to its receptor, IP_3R, yielding a release of calcium from its internal SR stores into the cytoplasm. Therefore, any changes in IP_3 levels can change the amount of intracellular calcium, because of release from the SR [36]. Another protein known as smooth endoplasmic reticular calcium ATPase (SERCA) is found within the SR membrane and is responsible for transporting calcium back into the SR. Decreases in SERCA activity could reduce the return of calcium to internal stores,

thus allowing a buildup of [Ca^{2+}]i in the cytoplasm and a reduction in Ca^{2+} concentration within the SR [36]. Lastly, the focus of this study are the Cav1.1 channels which are found along the sarcolemmal membrane and also in t-tubules. Changes in voltage along the t-tubules allows for a conformational change that affects ryanodine receptors within the SR allowing for calcium release, this in turn leads to excitation contraction coupling (ECC). Any changes in the Cav1.1 channel abundance or activity may lead to changes in the release of calcium from the SR [36]. Because ERG1a is a membrane bound protein detected on cardiac t-tubules [21, 37] and in the I-band of skeletal muscle where t-tubules are located (unpublished data, Zampieri and Pond), we thought it would be possible for ERG1a to have an effect on the L-type voltage-gated calcium channel Cav1.1. Cav1.1 is specific to the skeletal muscle membrane and is accepted to be the voltage sensor for excitation contraction coupling (ECC) in this tissue. Cav1.2 and 1.3 have not been reported in skeletal muscle, but are detected in cardiac muscle and adrenal glands, respectively. Cav1.1 works by sensing an action potential that moves down the t-tubules. Once this action potential is recognized, the Cav1.1 channel undergoes a conformational change which allows it to interact physically with the ryanodine receptors to release calcium from stores in the sarcoplasmic reticulum [28, 30, 38, 39]. This calcium release initiates ECC. Once ECC has occurred, reuptake of calcium into the SR occurs SERCA [38]. In a 2016 study by Sultana and colleagues reported that during maturation an embryological *Cav1.1* splice variant, that excludes exon 29 of *Cav1.1* (*Cav1.1e*), was found. After maturation this splice variant is replaced by an adult splice variant that includes exon 29 [28, 40]. It is suggested that the embryological splice variant differs from the adult in that it is much more sensitive to

voltage changes and spends an increased amount of time in the “open” state. Because it remains in the open state longer, Cav1.1e conducts much larger calcium currents as opposed to its adult counterpart. This small change in the channel’s structure allows calcium to be better regulated in adult muscle as opposed to developing muscle [40]. However, skeletal muscle is always adapting to demand and the Sultana study noted that knockout of Cav1.1e appeared to have effects on skeletal muscle similar to that of endurance training. Further investigation revealed Cav1.1e affected muscle fiber type composition in mice, causing an increase in slow type muscle fibers. Consequences of this change include: reduced tetanic, maximal twitch and grip force. Additionally, Cav1.1e and its increase in calcium flux appears to cause mitochondrial damage [34]. For this reason it is reasonable for us to hypothesize that Cav1.1 or its variant may produce an increase of calcium from internal stores. However, our investigation revealed that neither the Cav1.1 nor the Cav1.1e channel is affected by the presence of ERG1a. However, it is still possible that ERG1a affects Cav1.1 channel kinetics. This study is beyond the scope of this project and will be conducted in collaboration with a lab that focuses on electrophysiology.

Another possibility is that ERG1a affects calcium levels by modulation of IP_3. A previous study done by Perez-Neut [32] used a HERG activator (NS1643) on $SkBr_3$ breast cancer cells and found that indeed HERG activation leads to an increase in $[Ca^{2+}]i$ which promotes UPP activation and degradation of the cell cycle regulator protein, cyclin E2. Furthermore, activation of HERG via NS1643 hyperpolarized the membrane potential of the $SkBr_3$ cells which are otherwise non-excitable. Their report suggested that hyperpolarization may perhaps increase intracellular negative charge

leading to the entry of positively charged calcium into the cells. By blocking voltage gated calcium channels using $CoCl_2$ and activating HERG, a large increase in $[Ca^{2+}]i$ was discovered, these results suggested to them that the calcium entry was not a result of voltage gated calcium channel activity. Instead, they hypothesized that the inositol signaling pathway (IP_3) may have some effect on calcium entry. This data along with our own suggest that the Cav1.1 channel is not involved with this increase in $[Ca^{2+}]i$. Indeed, our lab now has preliminary data which suggests that intracellular calcium stores are involved in the increased $[Ca^{2+}]i$ (unpublished data, Pratt, Hockerman and Pond).

We were also able to demonstrate that in the presence of HERG1A, myotubes had an increased amount of calpain activity. At this time it is not possible to discern if calpains 1 and 2 are modulated differently and, if so, how. That is, is one of these isoforms transcribed or translated more than the other? Or is one activated more so than the other as a result of different effects on localized calcium concentration? The calpain system is complicated, and the activation of calpains is disputed. One thing that is agreed upon is that calpains must be autocatalyzed in order to be activated, specifically, on the N terminus [13, 16, 41, 42]. Indeed, the autolysis can be noted in our immunoblots (Figure 13-15) where multiple bands are seen [43]. The largest amount of controversy however concerns how calpains are activated. Calpain 1 has been shown to be at half maximal activity at low Ca^{2+} concentration (3-50 µM) while Calpain 2 reaches half maximal activity at higher concentrations (400-800 µM). Taken together, our lab's unpublished data showing that HERG1A expression in C2C12 myotubes yields an increase in $[Ca^{2+}]i$ combined with the results reported here which show that HERG1A

expression produces increased calpain activity, suggest that HERG1A is increasing calpain activity by increasing intracellular calcium concentration. However, it is possible that there is an increased abundance of calpain 1 and/or calpain 2 protein(s) or that there is a decrease in the abundance of the native calpain inhibitor calpastatin.

Calpains 1 and 2 are known as “conventional” calpains and are found throughout the body. Here we report a decrease in calpain 2 protein abundance in C2C12 myotubes in response to HERG1A expression while calpain 1 shows no detectable change in protein abundance. These data are aligned with the quantitative PCR data which demonstrate that there is no change in transcription of calpain 1 or 2 genes. Indeed, one would expect there to be no increase in calpain proteins without an increase in gene expression, although there could still be an increase in the protein as a result of decreased proteolysis. Because we see a decrease in calpain 2 without a change in transcription of that gene, we can speculate that the calpain 2 protein may be undergoing an increased level of degradation. Is it possible that the HERG1A protein is increasing ubiquitin proteasome proteolysis of calpain 2?

Calpains 1 and 2 are known to be upregulated during skeletal muscle atrophy caused by hind limb suspension, in a 2015 article by Shenkman and colleagues they inhibited calpain activity using the calpain inhibitor PD150606 [44]. Their results demonstrated that blocking calpain activity reduced the activation of calpain 1 gene expression and attenuated skeletal muscle atrophy. *Mafbx*/ATROGIN expression was also decreased in their experiments, however, there was no change in MURF1 expression, suggesting that although calpains affect *Mafbx* gene expression they have no effect on *Murf1*. In 2006, Fareed and colleagues [7] reported that calpain inhibition

also deterred muscle proteolysis induced by sepsis, however, they reported that this was independent of *Mafbx* and *Murf1*/ATROGIN gene expression. Interestingly, the Pond and Hannon labs showed that *Merg1a* expression in mouse skeletal muscle increased *Murf1* transcription and translation, but not that of *Mafbx*/ATROGIN [25]. The data suggest that ERG1A indeed has an effect on expression of UPP components, but does not suggest any connection with calcium up-regulation or increased calpain activity. Indeed, we find no report describing any calcium dependence by the UPP. Indeed, calpains are known to degrade skeletal muscle anchor proteins (e.g., titin, α-actinin, etc.) and, thereby release contractile proteins (i.e., actin and myosin) which are then degraded by the UPP [15, 45, 46]. We suggest that ERG1a may participate in the coordination of this effort by affecting both UPP and calpain activities.

Our results have shown that not only does calpain 2 protein abundance decrease, but calpain 3 protein abundance decreases as well. Calpain 3 is skeletal muscle specific and the absence or reduction of this protein leads to limb-girdle muscular dystrophy type 2A (LGMD2A) in humans [13, 41, 42, 47-50]. It is also interesting in that its regulation is not controlled solely by calcium but also by sodium concentrations; however, the physiological relevance of this discovery is debated [42, 51]. *In vitro* it has been shown that the Ca^{2+} concentration needed for calpain 3 to become completely active (in the absence of sodium) is 0.1mM. Whereas in the absence of calcium the Na^{+} concentration needed is much larger for activation, being 100mM. However, when both ions are present they act together and decrease the concentration needed for either ion for calpain activation [37]. *In vivo* experiments have been done to observe the Ca^{2+} concentration that is necessary to cause autolysis

(activation) in skeletal muscle tissue. The findings concluded that increased levels of calcium (200nM) were sufficient to autolyze ~20% of endogenous calpain 3 in a resting muscle fiber. The calpain activity, however, was dependent on the exposure duration and the presence of ATP. If the Ca^{2+} concentration became high enough, then ATP was not needed. It appears that the ATP increased the calpain 3 sensitivity to Ca^{2+} [49, 50]. It has been suggested, using calpain 3 knock out mice, that calpain 3 acts upstream of the UPP, although it is uncertain if calpain 3 directly cleaves proteins to make them accessible for ubiquitination [47]. What makes calpain 3 interesting is that it is not only known to break down proteins, but also takes part in remodeling of the sarcomere in response to cellular damage such as atrophy [42, 47]. It is proposed that calpain 3 is actually localized to the myofibrillar structure. *In vitro* it has been reported that calpain 3 targets include Z-disk proteins such as titin, filamin C, talin, and myosin light chain 1. This is supportive of a role for calpains in sarcomeric remodeling in response to cellular damage. In a report by Murphy and colleagues [41] they found that in response to eccentric exercise calpain 3 is autolyzed (activated). This would mean that calpain 3 is responding to the accumulation of minor damage to the sarcomere resulting from exercise by remodeling/repairing the structure; this occurrence is absent from those with LGMD2A. In a second report in 2010 Murphy [46] mentions that calpain 3 is not detected until later in development, following myoblast proliferation and fusion, this could explain why LGMD2A is a late onset disease (20-40 years of age), accumulated damage is not repaired due to the absence of calpain 3, leading to muscle wasting. Evidence has shown that the absence of calpain 3 may lead to a reduction in protein turnover and cause the accumulation of proteins that are damaged or misfolded. An

increase in misfolded and damaged proteins can lead to cellular stress. Indeed, studies have revealed an increase in heat shock proteins in response to the absence of calpain 3. This in turn may lead to cellular stress and toxicity, thus leading to muscle pathology (i.e., atrophy, dystrophy) [47, 52].

Calpastatin is a native calpain inhibitor which assists in maintaining calpain activity by inhibiting conventional calpains 1 and 2, but not calpain 3. A decrease in calpastatin protein decreases the ability of calpains to be regulated by inhibition. Calpastatin requires calcium in order to bind to calpains, but the concentration that is required is dependent on the calpain type [15]. When calcium concentrations rise, calpain activity is increased, thus calpastatin is needed to regulate their activity [13]. In our investigation of calpastatin the decrease in its protein abundance correlates with our calpain activity results. That is, in the absence of calpastatin, it would be expected to see an increase in calpain activity because it is no longer being inhibited by calpastatin.

In summary, our results suggest that voltage gated calcium channels are in fact not the cause of HERG1A-modulated increases in $[Ca^{2+}]i$. It is possible, therefore, that $[Ca^{2+}]i$ is affected by a different mechanism such as a change in IP_3 abundance or the ability of SERCA to reuptake calcium into the SR. We also provide evidence that ERG1a increases calpain activity in myotubes, likely resulting from the increase in $[Ca^{2+}]i$. Our observations of decreased calpain 2 and 3 abundance could be a result of their degradation, perhaps resulting from a feedback loop to decrease proteolysis despite or because of the increased calcium concentration. The decrease in calpain 3 may also be related to a decreased ability to remodel the sarcomere after atrophy, however, this possibility would require much additional investigation. Furthermore, the

decrease in calpastatin protein abundance may contribute to the increase in calpain activity that may also result from increased calcium concentration. Overall, our results suggest that HERG1A modulates intracellular calcium and calpain activity. Indeed, its interaction with calcium and calpains may work upstream of the UPP, and indeed modulate the UPP, having a multi-faceted modulatory effect on skeletal muscle atrophy. Indeed, ERG1a will likely never be a target for pharmacological treatments of atrophy, however, continuing study of this protein may reveal other possible targets to combat atrophy.

REFERENCES

[1] Frontera WR, Ochala J. Skeletal muscle: a brief review of structure and function. Calcif Tissue Int. 2015;96:183-95.

[2] Bonaldo P, Sandri M. Cellular and molecular mechanisms of muscle atrophy. Dis Model Mech. 2013;6:25-39.

[3] Bodine SC, Baehr LM. Skeletal muscle atrophy and the E3 ubiquitin ligases MuRF1 and MAFbx/atrogin-1. Am J Physiol Endocrinol Metab. 2014;307:E469-84.

[4] Baoge L, Van Den Steen E, Rimbaut S, Philips N, Witvrouw E, Almqvist KF, et al. Treatment of skeletal muscle injury: a review. ISRN Orthop. 2012;2012:689012.

[5] Lynch GS, Ryall JG. Role of beta-adrenoceptor signaling in skeletal muscle: implications for muscle wasting and disease. Physiol Rev. 2008;88:729-67.

[6] Derbre F, Ferrando B, Gomez-Cabrera MC, Sanchis-Gomar F, Martinez-Bello VE, Olaso-Gonzalez G, et al. Inhibition of xanthine oxidase by allopurinol prevents skeletal muscle atrophy: role of p38 MAPKinase and E3 ubiquitin ligases. PLoS One. 2012;7:e46668.

[7] Fareed MU, Evenson AR, Wei W, Menconi M, Poylin V, Petkova V, et al. Treatment of rats with calpain inhibitors prevents sepsis-induced muscle proteolysis independent of atrogin-1/MAFbx and MuRF1 expression. Am J Physiol Regul Integr Comp Physiol. 2006;290:R1589-97.

[8] Guasconi V, Puri PL. Epigenetic drugs in the treatment of skeletal muscle atrophy. Curr Opin Clin Nutr Metab Care. 2008;11:233-41.

[9] Han HQ, Mitch WE. Targeting the myostatin signaling pathway to treat muscle wasting diseases. Curr Opin Support Palliat Care. 2011;5:334-41.

[10] Hemmati-Brivanlou A, Kelly O, Melton D. Follistatin, an antagonist of activin, is expressed in the Spemann organizer and displays direct neuralizing activity. Cell. 1994;77:283-95.

[11] Smith RC, Lin BK. Myostatin inhibitors as therapies for muscle wasting associated with cancer and other disorders. Curr Opin Support Palliat Care. 2013;7:352-60.

[12] Stoka V, Turk V, Turk B. Lysosomal cathepsins and their regulation in aging and neurodegeneration. Ageing Res Rev. 2016;32:22-37.

[13] Sorimachi H, Ono Y. Regulation and physiological roles of the calpain system in muscular disorders. Cardiovasc Res. 2012;96:11-22.

[14] Neuhof C, Neuhof H. Calpain system and its involvement in myocardial ischemia and reperfusion injury. World J Cardiol. 2014;6:638-52.

[15] Goll DE, Neti G, Mares SW, Thompson VF. Myofibrillar protein turnover: the proteasome and the calpains. J Anim Sci. 2008;86:E19-35.

[16] Smith IJ, Lecker SH, Hasselgren PO. Calpain activity and muscle wasting in sepsis. Am J Physiol Endocrinol Metab. 2008;295:E762-71.

[17] Ma L, Chu W, Chai J, Shen C, Li D, Wang X. ER stress and subsequent activated calpain play a pivotal role in skeletal muscle wasting after severe burn injury. PLoS One. 2017;12:e0186128.

[18] Carlisle C, Prill K, Pilgrim D. Chaperones and the Proteasome System: Regulating the Construction and Demolition of Striated Muscle. Int J Mol Sci. 2017;19.

[19] Lehman W, Craig R, Vibert P. Ca2+-induced tropomyosin movement in Limulus thin filaments revealed by three-dimensional reconstruction. Nature. 1994;368:65.

[20] Vandenberg JI, Perry MD, Perrin MJ, Mann SA, Ke Y, Hill AP. hERG K(+) channels: structure, function, and clinical significance. Physiol Rev. 2012;92:1393-478.

[21] Jones EM, Roti Roti EC, Wang J, Delfosse SA, Robertson GA. Cardiac IKr channels minimally comprise hERG 1a and 1b subunits. J Biol Chem. 2004;279:44690-4.

[22] Lees-Miller J, Kondo C, Wang L, Duff HJ. Electrophysiological Characterization of an Alternatively Processed ERG K+ Channel in Mouse and Human Hearts. Circulation Research. 1997;81:719-26.

[23] London B, Trudeau MC, Newton KP, Beyer AK, Copeland NG, Gilbert DJ, et al. Two isoforms of the mouse ether-a-go-go-related gene coassemble to form channels with properties similar to the rapidly activating component of the cardiac delayed rectifier K+ current. Circulation Research. 1997;81:870-8.

[24] Wang X, Hockerman GH, Green HW, 3rd, Babbs CF, Mohammad SI, Gerrard D, et al. Merg1a K+ channel induces skeletal muscle atrophy by activating the ubiquitin proteasome pathway. FASEB J. 2006;20:1531-3.

[25] Pond AL, Nedele C, Wang WH, Wang X, Walther C, Jaeger C, et al. The mERG1a channel modulates skeletal muscle MuRF1, but not MAFbx, expression. Muscle Nerve. 2014;49:378-88.

[26] Glickman M, Ciechanover A. The Ubiquitin-Proteasome Proteolytic Pathway:

Destruction for the Sake of Construction. Physiological Reviews. 2002;82:373-428.

[27] Araya R, Liberona JL, Cárdenas JC, Riveros N, Estrada M, Powell JA, et al. Dihydropyridine Receptors as Voltage Sensors for a Depolarization-evoked, IP3R-mediated, Slow Calcium Signal in Skeletal Muscle Cells. The Journal of General Physiology. 2003;121:3-16.

[28] Bannister RA, Beam KG. Ca(V)1.1: The atypical prototypical voltage-gated Ca(2)(+) channel. Biochim Biophys Acta. 2013;1828:1587-97.

[29] Carrasco MA, Riveros N, J. Ro, Mu¨ ller M, Torres F, Pineda J, et al. Depolarization-induced slow calcium transients

activate early genes in skeletal muscle cells. American Journal of Physiology - Cell Physiology. 2003;284:C1438-C47.

[30] Catterall WA. Voltage-gated calcium channels. Cold Spring Harb Perspect Biol. 2011;3:a003947.

[31] Zhang S, Fritz N, Ibarra C, Uhlen P. Inositol 1,4,5-trisphosphate receptor subtype-specific regulation of calcium oscillations. Neurochem Res. 2011;36:1175-85.

[32] Perez-Neut M, Shum A, Cuevas BD, Miller R, Gentile S. Stimulation of hERG1 channel activity promotes a calciumdependent

degradation of cyclin E2, but not cyclin E1, in breast

cancer cells. Oncotarget. 2015;6:1631-9.

[33] Schlick B, Flucher BE, Obermair GJ. Voltage-activated calcium channel expression profiles in mouse brain and cultured hippocampal neurons. Neuroscience. 2010;167:786-98.

[34] Sultana N, Dienes B, Benedetti A, Tuluc P, Szentesi P, Sztretye M, et al. Restricting calcium currents is required for correct fiber type specification in skeletal muscle. Development. 2016;143:1547-59.

[35] Curran M, Splawski I, Timothy KW, Vincent GM, Green ED, Keating MT. A Molecular Basis for Cardiac Arrhythmia: HERG Mutations Cause Long QT Syndrome. Cell. 1995;80:795-803.

[36] Clapham DE. Calcium signaling. Cell. 2007;131:1047-58.

[37] Rasmussen HB, Moller M, Knaus H, Jensen BS, Olesen S, Jorgensen NK. Subcellular localization of the delayed rectifier K channels KCNQ1 and

ERG1 in the rat heart. American Journal of Physiology Hear and Circulatory Physiology. 2003;286:H1300-H9.

[38] Calderon JC, Bolanos P, Caputo C. The excitation-contraction coupling mechanism in skeletal muscle. Biophys Rev. 2014;6:133-60.

[39] Csernoch L, Jacquemond V. Phosphoinositides in Ca(2+) signaling and excitation-contraction coupling in skeletal muscle: an old player and newcomers. J Muscle Res Cell Motil. 2015;36:491-9.

[40] Tuluc P, Molenda N, Schlick B, Obermair GJ, Flucher BE, Jurkat-Rott K. A CaV1.1 Ca2+ channel splice variant with high conductance and voltage-sensitivity alters EC coupling in developing skeletal muscle. Biophys J. 2009;96:35-44.

[41] Murphy RM, Goodman CA, McKenna MJ, Bennie J, Leikis M, Lamb GD. Calpain-3 is autolyzed and hence activated in human skeletal muscle 24 h following a single bout of eccentric exercise. J Appl Physiol (1985). 2007;103:926-31.

[42] Ono Y, Ojima K, Shinkai-Ouchi F, Hata S, Sorimachi H. An eccentric calpain, CAPN3/p94/calpain-3. Biochimie. 2016;122:169-87.

[43] Li H, Thompson VF, Goll DE. Effects of autolysis on properties of mu- and m-calpain. Biochim Biophys Acta. 2004;1691:91-103.

[44] Shenkman BS, Belova SP, Lomonosova YN, Kostrominova TY, Nemirovskaya TL. Calpain-dependent regulation of the skeletal muscle atrophy following unloading. Arch Biochem Biophys. 2015;584:36-41.

[45] Goll DE, Thompson VF, Li H, Wei W, Cong J. The Calpain System. Physiological Reviews. 2003;83:731.

[46] Murphy RM. Calpains, skeletal muscle function and exercise. Clin Exp Pharmacol Physiol. 2010;37:385-91.

[47] Kramerova I, Kudryashova E, Venkatraman G, Spencer MJ. Calpain 3 participates in sarcomere remodeling by acting upstream of the ubiquitin-proteasome pathway. Hum Mol Genet. 2005;14:2125-34.

[48] Meznaric M, Writzl K. Limb-girdle muscular dystrophies: Different types and diagnosis. 2013.

[49] Murphy RM, Lamb GD. Endogenous calpain-3 activation is primarily governed by small increases in resting cytoplasmic [Ca^{2+}] and is not dependent on stretch. J Biol Chem. 2009;284:7811-9.

[50] Murphy RM, Vissing K, Latchman H, Lamboley C, McKenna MJ, Overgaard K, et al. Activation of skeletal muscle calpain-3 by eccentric exercise in humans does not result in its translocation to the nucleus or cytosol. J Appl Physiol (1985). 2011;111:1448-58.

[51] Ojima K, Ono Y, Ottenheijm C, Hata S, Suzuki H, Granzier H, et al. Non-proteolytic functions of calpain-3 in sarcoplasmic reticulum in skeletal muscles. J Mol Biol. 2011;407:439-49.

[52] Duguez S, Bartoli M, Richard I. Calpain 3: a key regulator of the sarcomere? FEBS J. 2006;273:3427-36.

VITA

Graduate School

Southern Illinois University

Clayton A. Whitmore

Claytonw726@gmail.com

Lincoln Land Community College

Associate of Science, May 2013

Illinois State University

Bachelor of Science, Molecular and Cell Biology, May 2015

Thesis Paper Title:

INVESTIGATION OF ERG1A POTASSIUM CHANNEL MODULATION OF CALPAIN ACTIVITY IN C2C12 MYOTUBES

Major Professor: Amber L. Pond